

Accepted Manuscript

Discovery of a potent dual ALK and EGFR T790M inhibitor

Jaebong Jang, Jung Beom Son, Ciric To, Magda Bahcall, So Young Kim, Seock Yong Kang, Mierzhati Mushajiang, Younho Lee, Pasi A. Jänne, Hwan Geun Choi, Nathanael S. Gray



PII: S0223-5234(17)30361-6

DOI: [10.1016/j.ejmech.2017.04.079](https://doi.org/10.1016/j.ejmech.2017.04.079)

Reference: EJMECH 9430

To appear in: *European Journal of Medicinal Chemistry*

Received Date: 6 March 2017

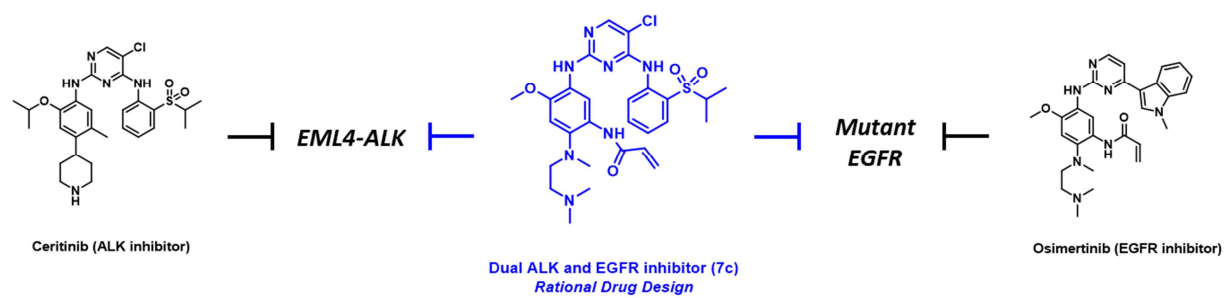
Revised Date: 27 April 2017

Accepted Date: 30 April 2017

Please cite this article as: J. Jang, J.B. Son, C. To, M. Bahcall, S.Y. Kim, S.Y. Kang, M. Mushajiang, Y. Lee, P.A. Jänne, H.G. Choi, N.S. Gray, Discovery of a potent dual ALK and EGFR T790M inhibitor, *European Journal of Medicinal Chemistry* (2017), doi: 10.1016/j.ejmech.2017.04.079.

This is a PDF file of an unedited manuscript that has been accepted for publication. As a service to our customers we are providing this early version of the manuscript. The manuscript will undergo copyediting, typesetting, and review of the resulting proof before it is published in its final form. Please note that during the production process errors may be discovered which could affect the content, and all legal disclaimers that apply to the journal pertain.

Graphical Abstract



Discovery of a Potent Dual ALK and EGFR T790M Inhibitor

Jaebong Jang^{a,c,1}, Jung Beom Son^{b,1}, Ciric To^{b,f}, Magda Bahcall^d, So Young Kim^g, Seock Yong Kang^g, Mierzhati Mushajiang^d, Younho Lee^g, Pasi A. Jänne^{b,d,e,h}, Hwan Geun Choi^{g,} and Nathanael S. Gray^{a,c,*}**

^aDepartment of Biological Chemistry & Molecular Pharmacology, ^bHarvard Medical School, Boston, Massachusetts 02115, United States

^cDepartment of Cancer Biology, ^dLowe Center for Thoracic Oncology and ^eBelfer Center for Applied Cancer Science, ^fDepartment of Medical Oncology, Dana-Farber Cancer Institute, Boston, Massachusetts 02215, United States

^gNew Drug Development Center, Daegu-Gyeongbuk Medical Innovation Foundation, Daegu 41061, Republic of Korea

^hDepartment of Medicine, Brigham and Women's Hospital, Boston, Massachusetts 02115, United States

* Corresponding author. E-mail: nathanael_gray@dfci.harvard.edu

** Corresponding author. E-mail: hgchoi@dgmif.re.kr

¹These authors contributed equally.

ABSTRACT

The mutational activations of anaplastic lymphoma kinase (ALK) and epidermal growth factor receptor (EGFR) are validated oncogenic events and the targets of approved drugs to treat non-small cell lung cancer (NSCLC). Here we report highly potent dual small molecule inhibitors of both ALK and EGFR, particularly the T790M mutant which confers resistance to first generation EGFR inhibitors. Dual ALK/EGFR inhibitors may provide an efficient approach to prevent resistance that arises as a consequence of clinically reported reciprocal activation mechanisms. Our lead compound **7c** displayed remarkable inhibitory activities against both ALK and EGFR in enzymatic and cellular assays. We demonstrate that **7c** is capable of recapitulating the signaling effects and antiproliferative activity of combined treatment with the approved ALK inhibitor ceritinib and T790M EGFR inhibitor osimertinib against patient-derived non-small cell lung cancer cell line, DFCI032 which harbors both EML4-ALK and activated EGFR.

Keywords

ALK, EGFR T790M, dual inhibitor, non-small cell lung cancer, rational drug design.

1. Introduction

Oncogenic mutations and translocations of receptor tyrosine kinases (RTKs) cause the development and progression of many cancers [1]. Small molecule drugs targeting dysregulated RTKs have distinct clinical benefits especially for genetically defined patient populations [2]. The anaplastic lymphoma kinase (ALK) and epidermal growth factor receptor (EGFR) have been well characterized as the leading oncogenic drivers of non-small cell lung cancer (NSCLC) [3]. In the past two decades, several wild-type and mutant-directed inhibitors of both ALK and EGFR have been developed. For example, the first-generation ALK inhibitor, crizotinib [4] and the first and second generation EGFR inhibitors, gefitinib [5], erlotinib [6] and afatinib [7] have been developed to treat NSCLC. Despite excellent response rates to these drugs, patients invariably relapse due to the emergence of drug resistant tumors. The second generation ALK inhibitors, ceritinib [8], alectinib [9] and brigatinib [10] and the third generation EGFR inhibitor, osimertinib [11-13] potentially overcome the secondary resistant mutations.

Despite extensive exploration of diverse chemotypes as inhibitors of ALK and EGFR, there have been no reports of small molecules that can act as dual inhibitors of both kinases. EGFR activation has been demonstrated as one of the compensatory resistance mechanisms of oncogenic ALK inhibition by small molecule inhibitors such as crizotinib, alectinib and ceritinib [14-16]. Additionally, with improved ability to perform single-cell sequencing there have been reports of tumors that harbor oncogenic alleles of both ALK and mutant EGFR concurrently [17-20].

Here we report the rational design, synthesis and biological evaluation of a dual inhibitor of ALK and EGFR, especially the T790M resistant mutant, that acts as a reversible ATP-competitive inhibitor with respect to ALK and as an irreversible, covalent inhibitor of the T790M mutant of EGFR.

2. Results and discussion

2.1 Rational drug design

Our study commenced by recognizing a structural similarity that exists between several of the known ALK inhibitors and EGFR inhibitors. The ALK inhibitors, ceritinib [21], TAE684 [22] and brigatinib [23] share a 2,4-disubstituted pyrimidine scaffold with the third generation EGFR inhibitors, osimertinib [11-13], WZ4002 [24] and rociletinib [25, 26]. Despite sharing the 2,4-disubstituted pyrimidine core, both ALK and EGFR inhibitors have distinct substituents that are critical to the recognition of their respective targets. In particular, the T790M EGFR inhibitors use a *meta*-acrylamide to enable the formation of a covalent bond with Cys797 located at the edge of the EGFR ATP binding pocket. The ALK inhibitors exploit an *ortho*-substituted isopropylsulfone (TAE684/ceritinib) or a dimethylphosphine oxide (brigatinib) to form a hydrogen bond with the catalytic Lys1150, which is critical to the binding affinity. Based on this structural analysis, we decided to combine both the acrylamide and *ortho*-substituted hydrogen bond acceptors with the 2,4-disubstituted pyrimidine scaffold with the aim of generating a dual ALK/EGFR inhibitor. (Figure 1) The *ortho*-alkoxy group at the C2-aniline substituent is a well-known functional group which is required to impart kinome-wide selectivity [21, 22]. For example, the methoxy group of WZ4002 led to improved selectivity for EGFR relative to its non-substituted analog, WZ3146 [24]. We also selected the methoxy group instead of a bulkier alkoxy group in our ALK/EGFR dual inhibitor because the isopropoxy substituent of ceritinib causes a loss of binding affinity for EGFR (Figure 3).

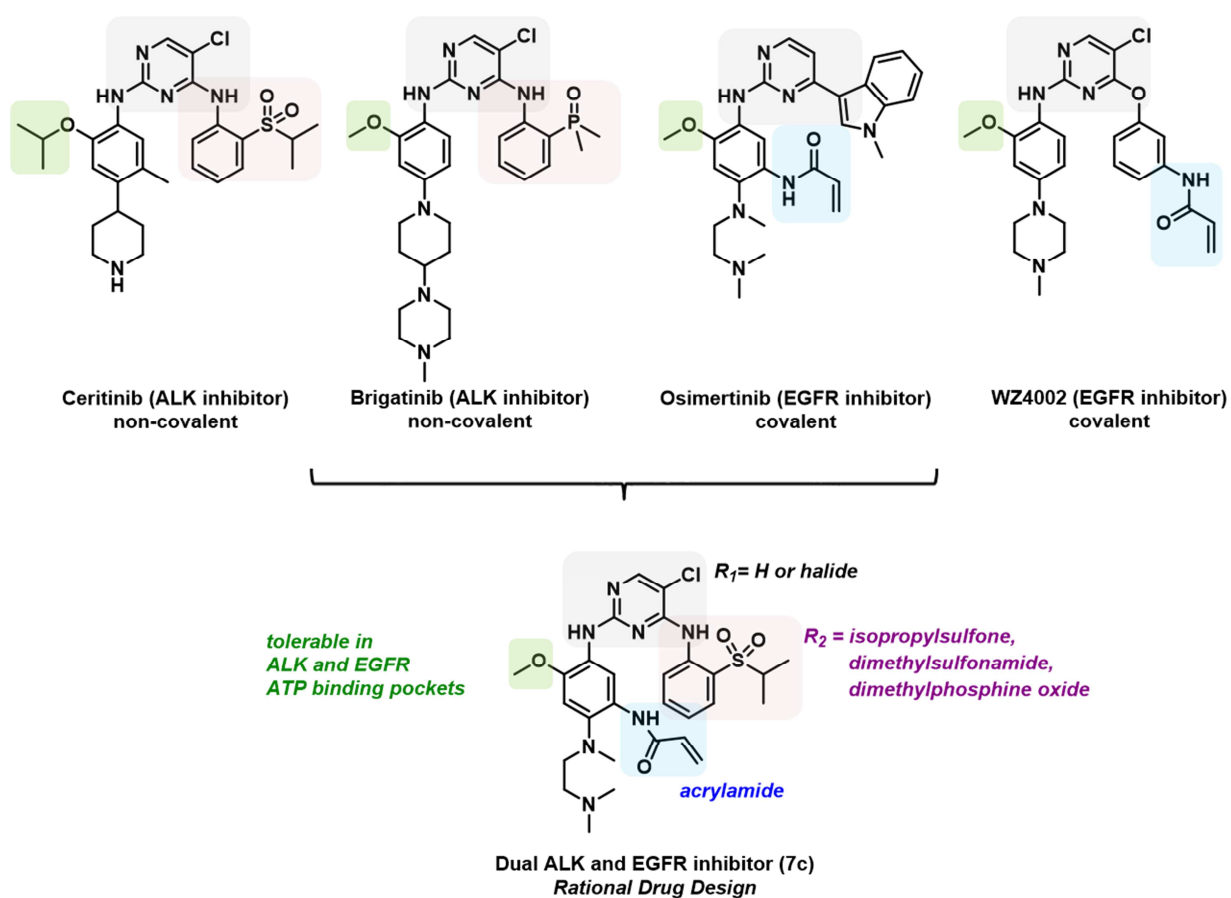


Figure 1. Rational design of dual ALK and EGFR inhibitor.

2.2 Structure-Activity Relationship

The potencies of newly synthesized compounds were first assessed biochemically using a *Z*-Lyte enzymatic assay for wild type ALK and an ATP-depletion (ADP-Glo) enzymatic assay for wild type EGFR, EGFR T790M and EGFR T790M/L858R. Compounds were subsequently evaluated using a proliferation assay employing Ba/F3 cells [27] transformed by either EML4-ALK, wild type EGFR or mutant EGFRs such as L858R, exon19del, L858R/T70M or exon19del/T790M. Furthermore, we utilized parental Ba/F3 cells grown in the presence of interleukin-3 (IL-3) to assess whether the compounds exhibited any general cytotoxicity.

First, we benchmarked our enzymatic and cellular ALK and EGFR assays using the ALK inhibitor, ceritinib and the EGFR inhibitors WZ4002 and osimertinib which share the 2,4-disubstituted pyrimidine core structure (Table 1). As expected, ceritinib exhibited excellent biochemical potency against wild type ALK with IC_{50} value of 20 nM and exhibited weak potency against wild type EGFR with IC_{50} value of $> 2 \mu\text{M}$. Interestingly, ceritinib also displayed potent inhibition of T790M and T790M/L858R EGFR mutants using the ADP-Glo assays, although less potent than the IC_{50} values measured for WZ4002 and osimertinib. This result was reproduced by a Z'-LYTE enzymatic assay (Invitrogen, Table S1). The observed biochemical potency of ceritinib for T790M EGFR was not observed in the Ba/F3 cellular assay (Table 2), highlighting the importance of tracking both the biochemical and cellular potencies. The two EGFR inhibitors displayed excellent potencies against all forms of EGFRs, especially T790M containing mutants ($IC_{50} = 5 \sim 7 \text{ nM}$), but displayed moderate to low potencies against wild type ALK ($IC_{50} = 990 \text{ nM}$ and 177 nM). These known drugs also showed similar trends in their cell growth inhibitory activities in the proliferation assays of Ba/F3 cells transformed with EML4-ALK, wild type EGFR and four different EGFR mutants (Table 2).

We next investigated which combination of functional groups are critical to achieving potent inhibition of ALK and EGFR, including the aforementioned *ortho*-hydrogen bond acceptor and the *meta*-acrylamide functional groups. We first synthesized and evaluated **7a** containing the *ortho*-isopropylsulfone at C4-aniline substituent and the *meta*-acrylamide at C2-aniline substituent of the pyrimidine core. **7a** displayed moderate enzyme inhibitory activities against wild type ALK, T790M EGFR and L858R/T790M EGFR with IC_{50} values of 103 nM, 26 nM and 86 nM respectively and it showed weak potency against wild type EGFR (Table 1). Consistent with the biochemical activities, **7a** showed moderate antiproliferative potencies

against mutant EGFR transformed Ba/F3 cells [EC_{50} = 78 nM (L858R), 195 nM (exon19del), 183 nM (T790M/L858R), 158 nM (exon19del/T790M)] while exhibiting weak proliferative inhibition of wild type EGFR (EC_{50} = 827 nM) as well as no meaningful inhibition against parental Ba/F3 cells ($EC_{50} \geq 5000$ nM). However, contrary to the biochemical assay, compound **7a** displayed poor antiproliferative activity against EML4-ALK transformed Ba/F3 cells which encouraged us to explore further the structure-activity relationships.

Previously, the C5-substituents of pyrimidine-based kinase inhibitors have been demonstrated as a key functional group for improving potency and kinase selectivity via the interaction with the gatekeeper residue [23, 28, 29]. Ceritinib, TAE684, brigatinib, and WZ4002 all possess a chlorine substituent at C5-pyrimidine which is required to achieve potent inhibition of ALK or EGFR. For WZ4002 an interaction of the C5-chlorine with the thioether of M790 was observed in the crystal structure and was critical to achieving selectivity for T790M over wild type EGFR [24, 30]. Similar to the known ALK and EGFR inhibitors, introduction of diverse halogens such as fluorine, chlorine and iodine at C5 of the pyrimidine core led to remarkable increases in inhibitory activities against both ALK and EGFRs (Tables 1 and 2). Especially compound **7c** containing a chlorine substituent, exhibited more than 300-fold improved antiproliferative activity against EML4-ALK transformed Ba/F3 cells. Moreover, inhibition of wild type EGFR and mutant EGFRs in enzymatic and cellular assays were improved by 15 ~ 30-fold, with maintenance of selectivity between wild type EGFR and mutant EGFRs. The fluorine derivative (**7b**) was roughly equipotent and had similar selectivity to **7c** but the iodine derivative (**7d**) showed slightly lower potencies against both ALK and EGFR while retaining selectivity for wild type and mutant EGFRs.

We next directed our attention to evaluate the combination of various *ortho*-hydrogen bond acceptors such as dimethylsulfonamide and dimethylphosphine oxide at C4-aniline with C5-halogen substituents (Table 1 and 2, **7e - 1**). The dimethylphosphine oxide analogs (**7e - 7h**) were slightly less potent against ALK than the isopropylsulfone analogs (**7a - 7d**) but, equipotent against wild type EGFR and mutant EGFRs in enzymatic assays and retained the potencies against mutant EGFR transformed Ba/F3 cells. However, these analogs totally lost their growth inhibitory activity against EML4-ALK transformed Ba/F3 cells. In contrast to the dimethylphosphine oxide, introduction of the dimethylsulfonamide group led to increases in inhibitory activities of both ALK and EGFRs in enzymatic and cellular assays (**7a** and **7i**) and when combined with the halogen substituents at C5 of the pyrimidine as in **7j - 7l**, biochemical and cellular potencies were similar to those of the isopropylsulfone analogs (**7b - 7d**). However, these analogs showed a slight cytotoxicity against parental Ba/F3 cells ($EC_{50} = 2.3 \sim 4.7 \mu\text{M}$) which led us to choose compound **7c** as a lead compound.

Compd. No.	R ₁	R ₂	ALK (IC ₅₀ , nM)		EGFR (IC ₅₀ , nM)	
			wt	wt	T790M	T790M/L858R
Ceritinib			20	2156	28	19
WZ4002			990	120	5	4
Osimertinib			177	114	5	7
7a	H		103	2480	26	86
7b	F		17	46	2	2
7c	Cl		18	151	2	4
7d	I		91	865	9	33

7e	H		695	149	5	35
7f	F		123	106	2	5
7g	Cl		40	65	2	12
7h	I		41	54	2	8
7i	H		31	307	4	12
7j	F		15	172	2	3
7k	Cl		17	204	2	4
7l	I		38	244	3	5

Table 1. Enzymatic Inhibitory Activities against ALK and EGFR.

Compd. No.	R ₁	R ₂	EML4-ALK (EC ₅₀ , nM)	EGFR (EC ₅₀ , nM)					Parental (EC ₅₀ , nM)
				wt	L858R	Del	T790M/L 858R	T790M/ Del	
Ceritinib			26	> 3000	3000	2500	2500	2660	> 5000
WZ4002			6258	989	26	68	31	27	> 5000
Osimertinib			1748	66	6	18	20	16	> 5000
7a	H		2182	827	78	195	183	158	> 5000
7b	F		20	25	2	5	5	5	> 5000
7c	Cl		7	32	4	6	6	5	> 5000

7d	I		87	240	19	47	22	20	> 5000
7e	H		> 5000	988	236	680	830	400	> 5000
7f	F		2506	178	68	157	162	74	> 5000
7g	Cl		961	68	21	44	45	30	> 5000
7h	I		2357	96	23	84	31	32	> 5000
7i	H		217	93	19	21	22	19	> 5000
7j	F		39	31	8	6	6	5	4661
7k	Cl		8	69	4	6	6	5	2904
7l	I		21	262	19	24	19	17	2270

Table 2. Antiproliferation Activities against EML4-ALK Ba/F3 and EGFR Ba/F3 Cells.

2.3 Characterization of compound **7c**

We next performed detailed characterization of **7c** including a molecular modeling study, kinome selectivity profile, effects on ALK and EGFR-dependent signaling pathways, antiproliferative activity on patient-derived NSCLC and pharmacokinetic profile in mouse.

To better rationalize the structural-basis for the observed dual inhibition of ALK and EGFR, we performed a molecular modeling based on the co-crystal structures of ALK and ceritinib (PDB 4MKC), wild type EGFR and osimertinib (PDB 4ZAU) and T790M EGFR and

WZ4002 (PDB 3IKA) (Figure 2). **7c** is predicted to bind to the ATP binding site similarly to ceritinib and WZ4002 making identical hydrogen bonds to the hinge residues Met1199 and Met793. We carefully investigated the binding modes of two distinct functional groups such as the *meta*-acrylamide in ALK and the *ortho*-isopropylsulfone in EGFR. The residue corresponding to the Cys797 in EGFR, which forms the covalent bond with the *meta*-acrylamide (Table S2), is the Asp1203 in ALK. We did not find an additional interaction between the *meta*-acrylamide of **7c** and the Asp1203, but it is well accommodated by this residue at the edge of the ATP binding pocket. On the other hand, ALK and EGFR have the same residues around the region of the binding pocket occupied by the *ortho*-isopropylsulfone, except for the DFG-1 residue (Gly1269 in ALK and Thr854 in EGFR), which creates similar binding pockets. As a result, the *ortho*-isopropylsulfone is positioned in proximity to the catalytic Lys745 in wild type EGFR and T790M mutant EGFR, which forms an additional hydrogen bond as observed in the ceritinib-ALK co-crystal structure.

(A)

(B)

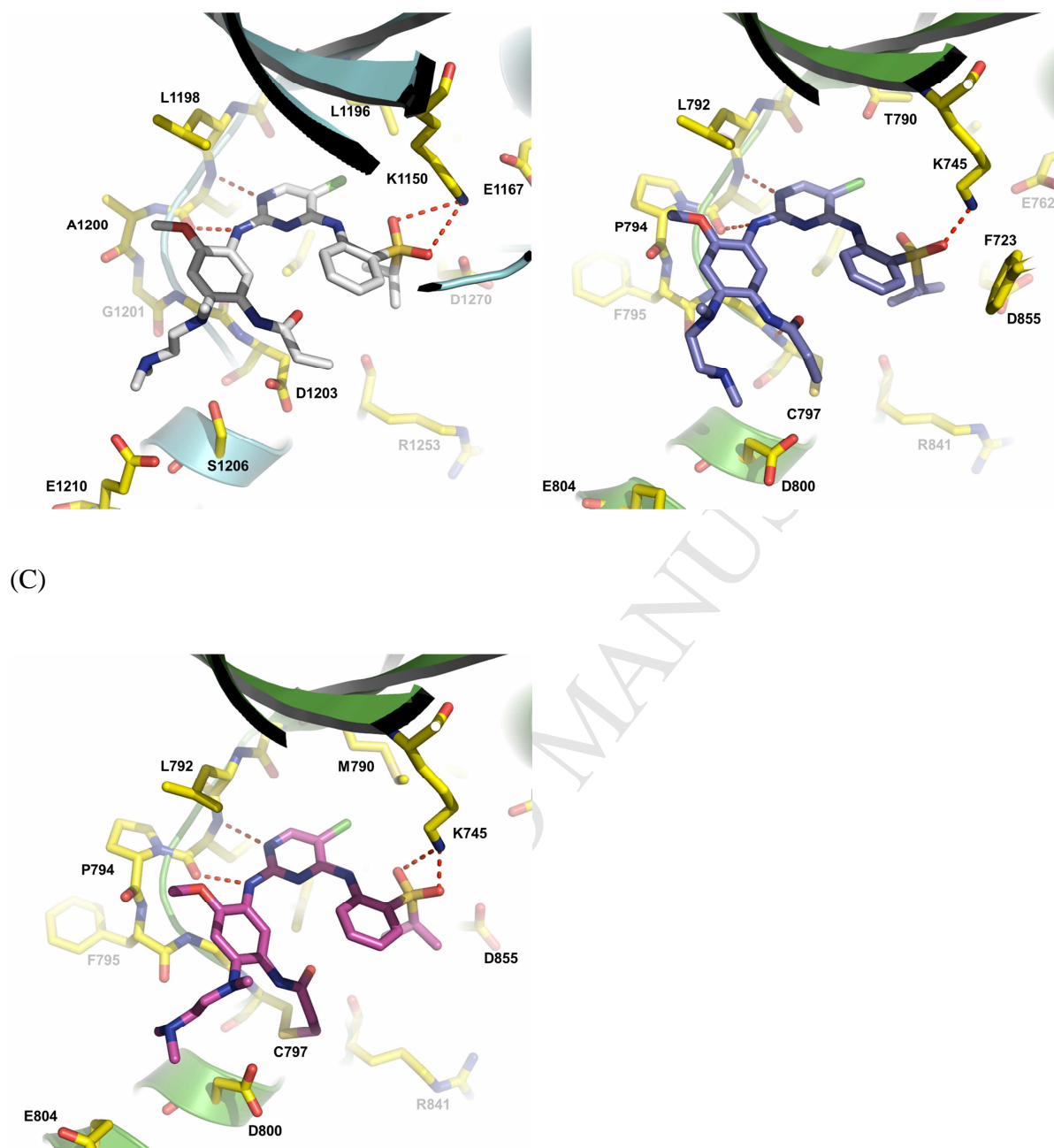
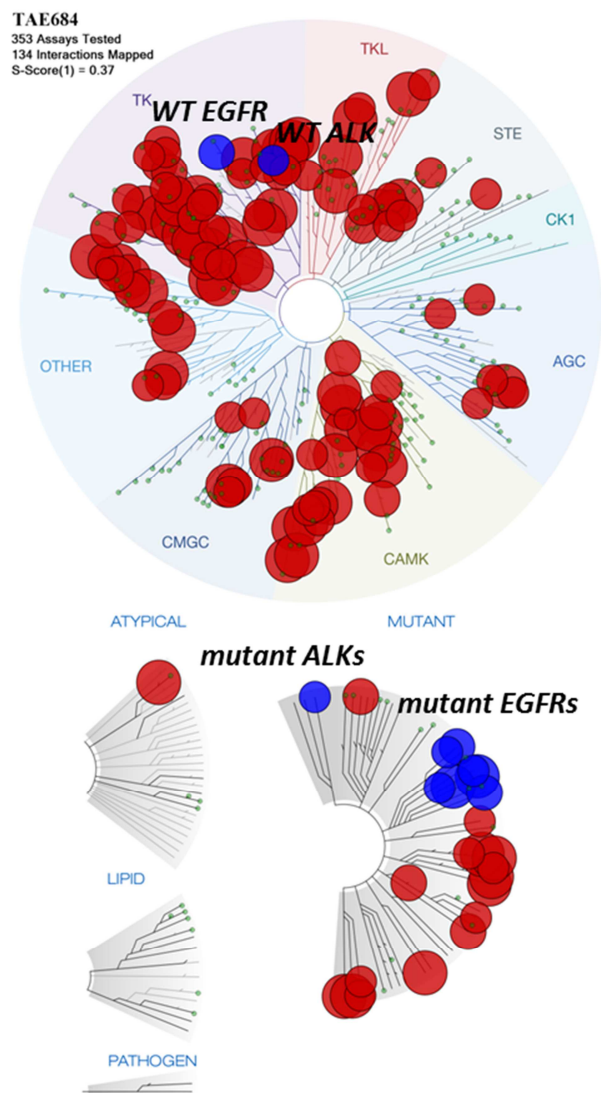


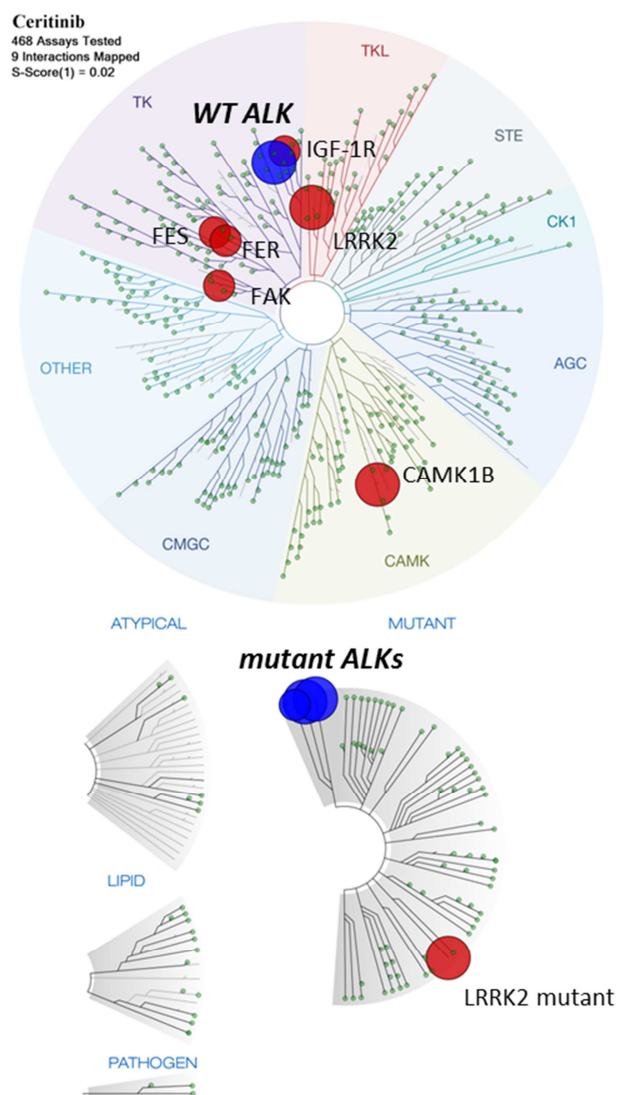
Figure 2. Molecular docking models of compound **7c** bound to (A) wild type ALK, (B) wild type EGFR and (C) T790M EGFR. Hydrogen bonds are indicated by dashed lines.

We assessed the kinase selectivity of **7c** using the KINOMEScan technology [DiscoverX] [31, 32] against a diverse panel of 468 kinases at a concentration of 1 μ M and compared it to the profiles obtained for both TAE684 (panel of 353 kinases) and ceritinib (Figure 3). Hydrogen bond acceptors such as sulfone, sulfonamide and phosphine oxide, are well known functional groups which interact with the conserved catalytic lysine. Installing these functional groups at *ortho*-position of C4-anilinopyrimidine leads to poor kinome selectivity. However, ceritinib, which has a bulky *ortho*-isopropoxy substituent at C2-anilinopyrimidine, achieved good kinase selectivity [S-score(1) = 0.02] even though it contains the *ortho*-isopropylsulfone at the C4-anilinopyrimidine, compared to TAE684 which has the *ortho*-methoxy group [S-score(1) = 0.37]. However, ceritinib lost affinity for EGFR proteins in KINOMEScan which encouraged us to retain the *ortho*-methoxy substituent of 2-anilinopyrimidine. Fortunately, **7c** displayed superior overall kinome selectivity [S-score(1) = 0.07] relative to TAE684, and as expected it still bound to both wild type and mutants ALK and EGFR. The profiling revealed a number of potential off-targets such as ErbB2, ErbB4, BTK and BLK, which have a cysteine residue at the same position as the Cys797 of EGFR [24], and several non-receptor tyrosine kinases (Table S3).

(A)



(B)



(C)

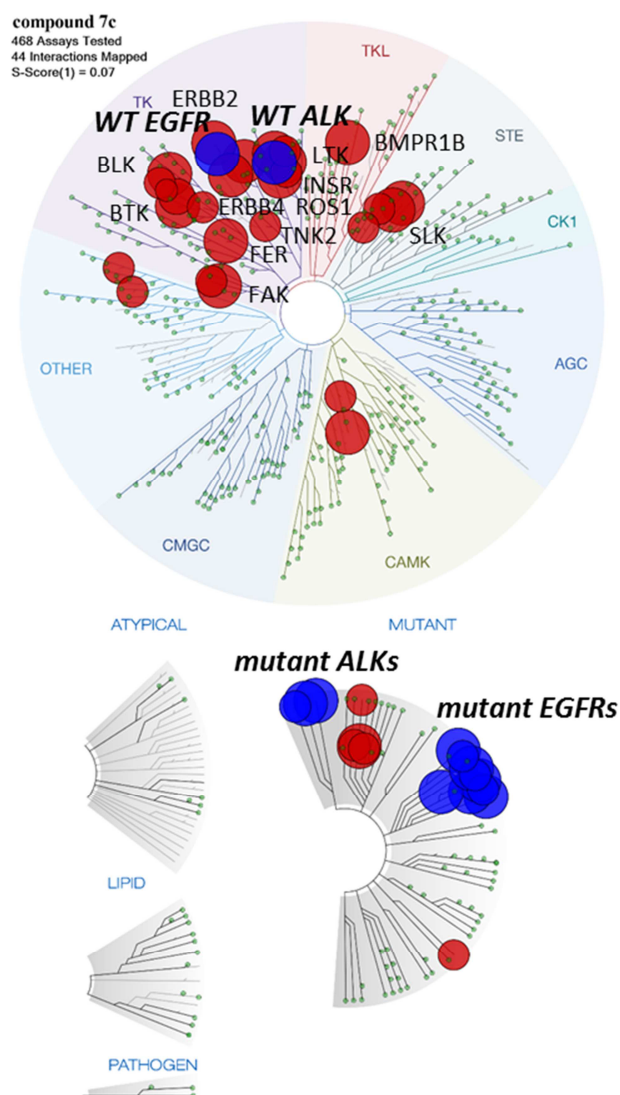


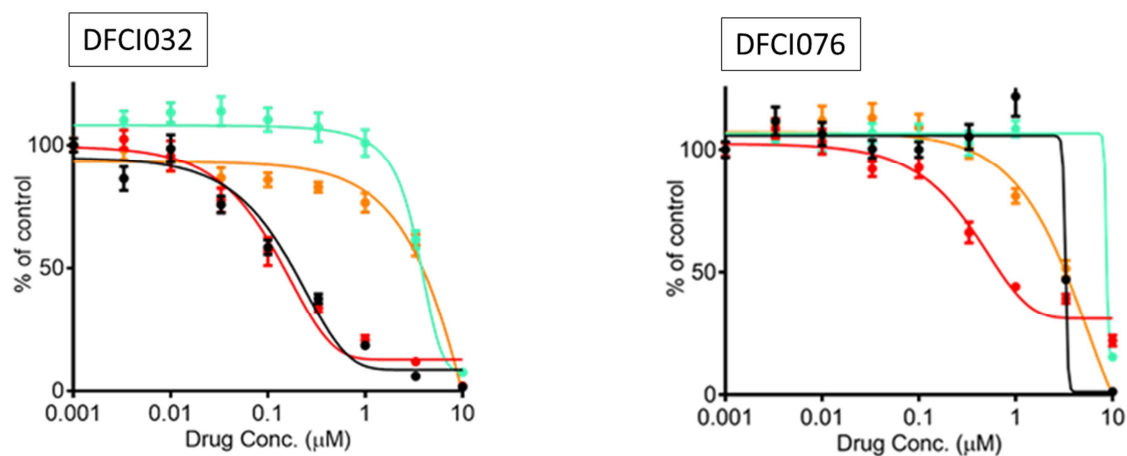
Figure 3. Kinome-wide selectivity profiles of (A) TAE684, (B) ceritinib and (C) compound **7c** at a 1 μ M concentration. Wild type and mutants ALK and EGFR are indicated by blue spots.

We investigated the cell growth inhibitory activity of **7c** against patient-derived lung cancer cell line, DFCI032, which harbors wild type EML4-ALK together with activated EGFR [33]. We also tested DFCI076 cell line, which harbors both activated EGFR and an L1152R mutation in the ALK kinase domain, which renders cells resistant to most ALK inhibitors [14, 34]

(Figure 4A and 4B). As expected, ceritinib or osimertinib alone were not able to efficiently inhibit the proliferation of DFCI032 ($EC_{50} = 4.44 \mu\text{M}$ and $4.73 \mu\text{M}$, respectively). In contrast, our lead compound **7c** exhibited remarkable inhibitory effect against DFCI032 cells with an EC_{50} value of $0.17 \mu\text{M}$, which is 25-fold more potent than ceritinib or osimertinib alone and equipotent to a 1:1 combination treatment of ceritinib and osimertinib ($EC_{50} = 0.19 \mu\text{M}$). On the other hand, the 1:1 combination of ceritinib and osimertinib was not able to efficiently inhibit the proliferation of DFCI076 due to the loss of ALK inhibition. **7c** was also less effective against DFCI076, but was 5-fold more potent than the 1:1 combination of ceritinib and osimertinib, which was presumably due to stronger ALK inhibition than ceritinib. This result strongly supports the ability of **7c** to inhibit both ALK and EGFR in a patient-derived cellular context, in good agreement with the engineered Ba/F3 cellular assays.

To assess the capability of **7c** to downregulate ALK and EGFR signaling pathways simultaneously in a cellular context, we performed Western blotting for phosphorylated ALK and EGFR as well as downstream signaling mediators such as Akt and ERK in DFCI032 cells (Figure 4C). Ceritinib and osimertinib suppressed phosphorylation of their primary target respectively but were not able to sufficiently reduce phosphorylation of Akt and ERK. On the other hand, the 1:1 combination of ceritinib and osimertinib effectively inhibited phosphorylation of both ALK and EGFR as well as Akt and ERK. Consistent with the cell growth inhibitory activity, **7c** alone also showed dual inhibition of ALK and EGFR phosphorylation which led to better suppression of both PI3K/Akt and MAPK/ERK pathways than the 1:1 combination of ceritinib and osimertinib.

(A)



(B)

Patient-derived cell line	EML4-ALK variant	Crizotinib sensitivity	Resistance mechanism	EC ₅₀ (μM)			
				Ceritinib	Osimertinib	7c	Ceritinib/Osimertinib (1:1)
DFCI032	1	Resistant	WT ALK TKD; EGFR activation	4.44	4.73	0.17	0.19
DFCI076	3	Resistant	ALK L1152R mutation; EGFR activation	3.49	7.93	0.82	3.21

(C)

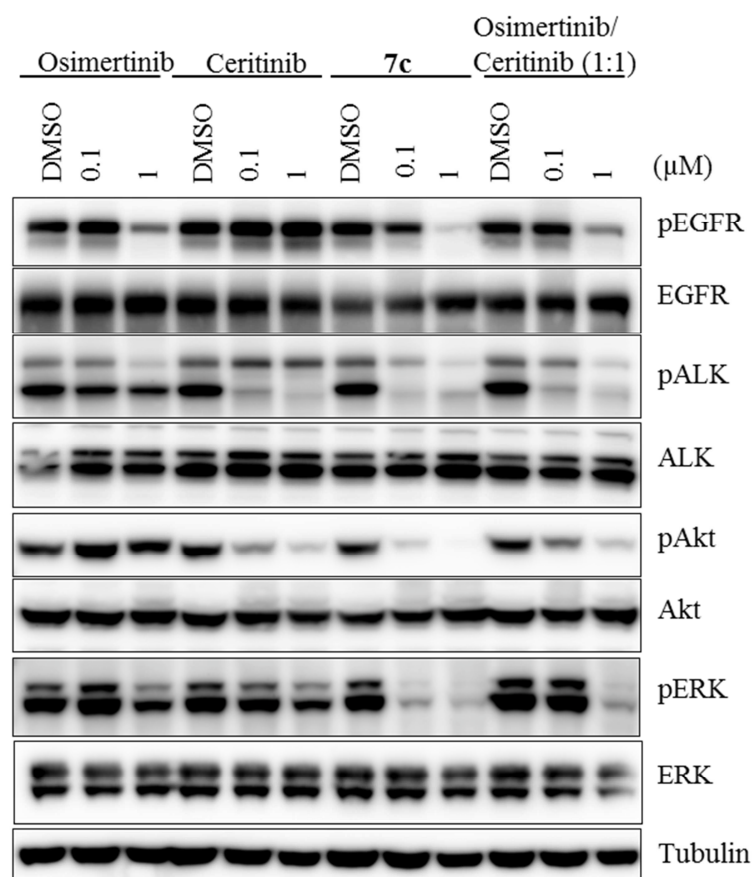


Figure 4. Profiles of compound **7c** in patient-derived NSCLC. (A) Dose-dependent cell growth curves of ceritinib (orange), osimertinib (cyan), compound **7c** (red) and the 1:1 combination of ceritinib and osimertinib (black) against DFCI032 and DCI076. (B) Cellular contexts of DFCI032 and DFCI076 and EC_{50} values. (C) Effects on phosphorylation of ALK, EGFR, Akt and ERK in DFCI032 cells.

We profiled the *in vitro* metabolic stability of newly synthesized compounds using human, dog, rat and mouse liver microsomes and we evaluated their ability to inhibit cytochrome P450 (CYP) *in vitro* (Table 3). Generally, the dimethylphosphine oxide analogs showed superior

microsomal stability and lower CYP enzyme inhibition than the corresponding isopropylsulfone analogs and the dimethylsulfonamide analogs which displayed 30 - 60 % inhibition of CYP 3A4 and approximately 20 % inhibition of other CYP enzymes. Our lead compound **7c** was not stable in liver microsomes of all species whereas corresponding dimethylphosphine oxide analog **7g** displayed good microsomal stability. This result was not surprising because the dimethylphosphine oxide analogs showed lower clog *P* values than the isopropylsulfone analogs and dimethylsulfonamide analogs.

Compd. No.	R ₁	R ₂	Cytochrome P450 inhibition (% of control)					Liver microsomal stability (% remaining after 30 min)				cLog <i>P</i> ^a
			1A2	2C9	2C19	2D6	3A4	Human	Dog	Rat	Mouse	
7a	H		80	90	87	67	40	5	48	22	8	3.9
7b	F		91	94	93	95	51	26	27	11	15	4.1
7c	Cl		89	83	86	90	44	16	17	11	12	4.7
7d	I		81	88	86	82	47	14	19	14	10	5.1
7e	H		84	90	>100	87	89	70	73	78	76	2.0
7f	F		>100	>100	>100	>100	>100	84	87	87	80	2.2
7g	Cl		93	>100	98	85	91	61	77	76	66	2.8
7h	I		91	>100	99	80	88	65	93	81	57	3.2

7i	H		82	88	85	79	56	10	50	6	5	3.9
7j	F		>100	88	91	>100	71	9	33	7	10	4.1
7k	Cl		87	59	75	88	39	11	31	13	23	4.6
7l	I		79	85	67	93	54	13	35	12	12	5.0

^aCalculated log *P* using ChemDraw Professional version 16.0.0.82.

Table 3. Metabolic Stability in Liver Microsome and Cytochrome P450 Enzyme Inhibition of Compound **7a-l**.

7c displayed reasonable mouse pharmacokinetic properties with a moderate $T_{1/2}$ of 1.25 hour and AUC_{last} value of 1551 ng·h/mL following an oral dose of 10 mg/Kg (Table 4A). Furthermore, 2 hours after an intravenous (2 mg/Kg) or an oral (10 mg/Kg) dose, **7c** showed higher lung exposure (2.36 μM and 4.64 μM) than plasma exposure (0.10 μM and 0.15 μM) which lasted for 8 hours (0.11 μM and 0.74 μM versus 0.00 μM and 0.01 μM). Despite low bioavailability (24 %), the preferential accumulation of **7c** in lung tissue over plasma would be advantageous to use in studying the effects of dual ALK/EGFR inhibition in murine models of lung cancer (Table 4B).

(A)

ID	route	dose (mg/Kg)	matrix	$T_{1/2}$ (hr)	T_{max} (hr)	C_{max} (ng/mL)	AUC_{last} (hr·ng/mL)	Cl_{obs} (mL/min/Kg)	$V_{ss,obs}$ (L/Kg)	F (%)
7c	IV	2	plasma	1.25		882	1287	28.99	2.66	
	PO	10	plasma		1.17	520	1551	114.54		24

(B)

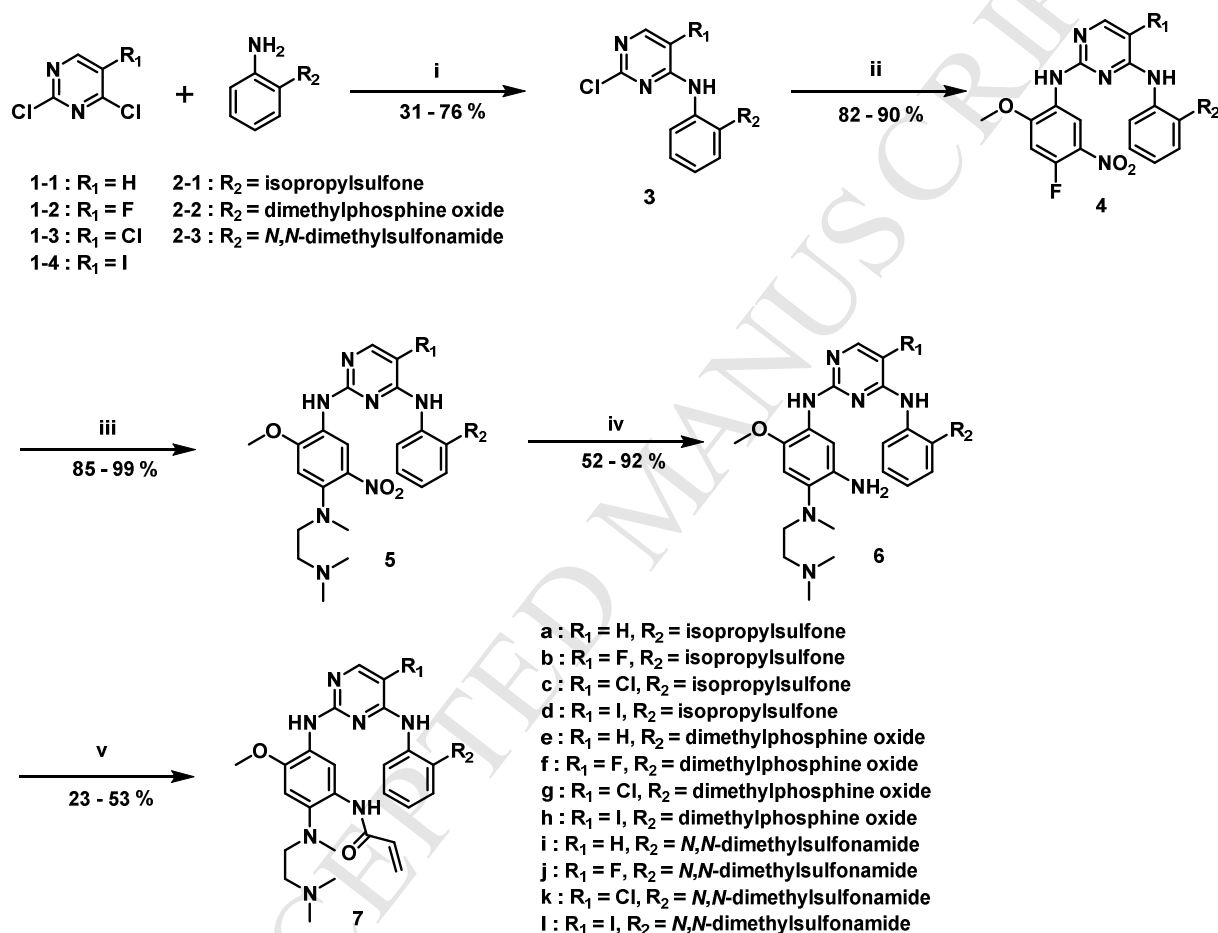
ID	matrix	route	dose (mg/Kg)	time (hr)	conc. (μ M)
7c	plasma	IV	2	2	0.10
		PO	10	2	0.15
		IV	2	8	0.00
		PO	10	8	0.01
7c	lung	IV	2	2	2.36
		PO	10	2	4.64
		IV	2	8	0.11
		PO	10	8	0.74

Table 4. (A) Pharmacokinetic Properties and (B) *In vivo* Lung Tissue Availability of Compound 7c.

2.4 Chemistry

The synthesis, which is described in scheme 1, followed well established synthetic routes for similar compounds [13, 21, 23]. All variations were made at the first nucleophilic aromatic substitution (S_NAr) reaction step using commercially available 2,4-dichloropyrimidine cores and three different anilines. Then, we performed a four-step reaction sequence to synthesize the isopropylsulfone and dimethylsulfoamide analogs (**7a - d** and **7i - l**) including two S_NAr

reactions, nitro-reduction and acrylamide formation to install the C2-aniline substituent. The dimethylphosphine oxide analogs (**7e - h**) were also made via similar route except for a Buchwald coupling which was employed to install the 4-fluoro-2-methoxy-5-nitroaniline at C2-position of pyrimidine.



(i) 2-1 and 2-3 : NaH, DMF/DMSO (9:1), 0 °C; 2-2 : K₂CO₃, DMF, 70 °C; (ii) 3a - d and 3i - l : 4-fluoro-2-methoxy-5-nitroaniline, TFA, 2-BuOH, 100 °C; 3e - h : 4-fluoro-2-methoxy-5-nitroaniline, Pd₂dba₃, Xphos, K₂CO₃, 2-BuOH; (iii) *N*¹,*N*¹,*N*²-trimethylethane-1,2-diamine, 1,4-dioxane, 80 °C; (iv) 5a - d and 5i - l : SnCl₂·2H₂O, HCl, EtOAc; 5e - h : Pd/C, H₂ gas, MeOH; (v) acryloyl chloride, sat. NaHCO₃/THF (1:1).

Scheme 1. Synthetic Routes for Compound **7a-l**.**3. Conclusion**

Based on our previous effort developing covalent T790M EGFR inhibitor, WZ4002, we have rationally designed and synthesized the potent dual inhibitor of ALK and EGFR, particularly the T790M resistant mutant, by combining the crucial functional groups of known ALK inhibitors ceritinib and brigatinib, and EGFR inhibitors WZ4002 and osimertinib, in the 2,4-diarylaminopyrimidine scaffold. This effort resulted in the identification of **7c** as a potent dual inhibitor of ALK and EGFRs, including T790M and L858R/T790M mutants, in biochemical assays with low nanomolar IC_{50} values, which was well correlated with cell growth inhibitory activities against EML4-ALK, wild type EGFR, L858R, exon19del, L858R/T790M or exon19del/T790M EGFR transformed Ba/F3 cells. Moreover, compound **7c** recapitulated the cell growth inhibitory activity observed upon combinatorial treatment with both ceritinib and osimertinib against the patient-derived NSCLC cell line, DFCI032 which harbors both EML4-ALK and activated EGFR, and inhibited the cellular phosphorylation of ALK and EGFR, as well as their downstream signaling proteins Akt and ERK. These results suggest that **7c** is a promising lead compound to develop advanced ALK and EGFR dual inhibitors. Further optimization of this scaffold to improve metabolic stability and kinome-wide selectivity is currently underway.

4. Experimental protocols

4.1 Chemistry

Starting materials, reagents and solvents were purchased from commercial suppliers and were used without further purification unless otherwise noted. All reactions were monitored using a Waters Acquity UPLC/MS system (Waters PDA $\epsilon\lambda$ Detector, QDa Detector, Sample manager – FL, Binary Solvent Manager) using Acquity UPLC® BEH C18 column (2.1 x 50 mm, 1.7 μ m particle size): solvent gradient = 90 % A at 0 min, 1 % A at 1.6 min; solvent A = 0.1 % formic acid in Water; solvent B = 0.1 % formic acid in Acetonitrile; flow rate : 0.6 mL/min. Reaction products were purified by flash column chromatography using CombiFlash®Rf with Teledyne Isco RediSep®Rf High Performance Gold or Silicycle SiliaSep™ High Performance columns (4 g, 12 g, 24 g, 40 g, or 80 g) and Waters HPLC system using SunFire™ Prep C18 column (19 x 100 mm, 5 μ m particle size): solvent gradient = 80 % A at 0 min, 10 % A at 25 min; solvent A = 0.035 % TFA in Water; solvent B = 0.035 % TFA in MeOH; flow rate : 25 mL/min. ¹H NMR spectra were recorded on 400 MHz and 500 MHz Bruker Avance III spectrometers and ¹³C NMR spectrum was recorded on 125 MHz Bruker Avance III spectrometer. The mass spectrometry data were measured in positive electrospray ionization (ESI) mode on LCMS-2020 system (Shimadzu, Tokyo, Japan). Chemical shifts are reported relative to methanol (δ = 3.30), chloroform (δ = 7.24) or dimethyl sulfoxide (δ = 2.50) for ¹H NMR and ¹³C NMR. Data are reported as (*br* = broad, *s* = singlet, *d* = doublet, *t* = triplet, *q* = quartet, *m* = multiplet).

4.1.1 Representative procedure for the synthesis of compounds **7a** - **7d** and **7i** - **7l**

2,5-Dichloro-N-(2-(isopropylsulfonyl)phenyl)pyrimidin-4-amine (3c). To a solution of 2-(isopropylsulfonyl)aniline (3.0 g, 15.1 mmol) in DMF (80 mL) was added sodium hydride (1.2 g, 30.1 mmol, 60 % in mineral oil) at 0 °C. After stirring for 30 min, 2,4,5-trichloropyrimidine was added to the reaction mixture followed by warming the mixture to room temperature. After stirring for 2 h, the reaction mixture was quenched with ice and diluted with excess water. The precipitate was filtered and the solid was dried by blowing nitrogen gas to obtain **3c** as an off-white solid (3.75 g, 72 %). ¹H NMR (500 MHz, DMSO-*d*₆) δ 9.81 (s, 1H), 8.56 (s, 1H), 8.33 - 8.31 (m, 1H), 7.89 (dd, *J* = 7.9, 1.5 Hz, 1H), 7.88 - 7.84 (m, 1H), 7.48 (td, *J* = 7.6, 1.2 Hz, 1H), 3.58 - 3.48 (m, 1H), 1.16 (d, *J* = 6.7, 6H); LC/MS (ESI) *m/z* 346.18 [M+H]⁺.

5-Chloro-N²-(4-fluoro-2-methoxy-5-nitrophenyl)-N⁴-(2-(isopropylsulfonyl)phenyl)pyrimidine-2,4-diamine (4c). To a suspension of 2,5-dichloro-*N*-(2-(isopropylsulfonyl)phenyl)pyrimidin-4-amine (**3c**) (1.0 g, 2.89 mmol) and 4-fluoro-2-methoxy-5-nitroaniline (0.565 g, 3.03 mmol) in 2-butanol (10 mL) was added trifluoroacetic acid (1.1 mL, 14.5 mmol). Then, the mixture was stirred at 80 °C for 6 h followed by cooling to room temperature. The resulting mixture was concentrated under reduced pressure and the residue was purified by flash column chromatography on silica gel (0 to 10 % MeOH in DCM) to give **4c** as a brown solid (1.23 g, 86 %). ¹H NMR (500 MHz, DMSO-*d*₆) δ 9.53 (s, 1H), 8.72 (s, 1H), 8.54 (d, *J* = 8.2 Hz, 1H), 8.44 (d, *J* = 7.3 Hz, 1H), 8.33 (s, 1H), 7.82 (dd, *J* = 7.9, 1.5 Hz, 1H), 7.62 - 7.55 (m, 1H), 7.37 - 7.31 (m, 2H), 3.95 (s, 3H), 3.50 - 3.40 (m, 1H), 1.16 (d, *J* = 6.7, 6H); LC/MS (ESI) *m/z* 496.36 [M+H]⁺.

5-Chloro-*N*²-(4-((2-(dimethylamino)ethyl)(methyl)amino)-2-methoxy-5-nitrophenyl)-*N*⁴-(2-(isopropylsulfonyl)phenyl)pyrimidine-2,4-diamine (**5c**). To a solution of 5-chloro-*N*²-(4-fluoro-2-methoxy-5-nitrophenyl)-*N*⁴-(2-(isopropylsulfonyl)phenyl)pyrimidine-2,4-diamine (**4c**) (0.800 g, 1.61 mmol) in dioxane (5 mL) was added *N*¹,*N*¹,*N*²-trimethylethane-1,2-diamine (0.640 mL, 4.84 mmol). The reaction mixture was stirred at 100 °C for 2 h. After completion of the reaction, the resulting mixture was concentrated under reduced pressure and purified by flash column chromatography on silica gel (0 to 20 % MeOH in DCM) to give **5c** as a sticky liquid (838 mg, 90 %) ¹H NMR (500 MHz, DMSO-*d*₆) δ 9.53 (s, 1H), 8.55 (s, 1H), 8.49 (br, 1H), 8.27 (s, 1H), 8.17 (br, 1H), 7.81 (dd, *J* = 7.9, 1.5 Hz, 1H), 7.60 - 7.51 (m, 1H), 7.34 - 7.29 (m, 1H), 6.84 (s, 1H), 3.90 (s, 3H), 3.49 - 3.40 (m, 1H), 3.40 - 3.24 (m, 2H), 2.88 (br, 2H), 2.83 (s, 1H), 2.47 (br, 6H), 1.16 (d, *J* = 6.7, 6H); LC/MS (ESI) *m/z* 578.59 [M+H]⁺.

*N*⁴-(5-Chloro-4-((2-(isopropylsulfonyl)phenyl)amino)pyrimidin-2-yl)-*N*¹-(2-(dimethylamino)ethyl)-5-methoxy-*N*¹-methylbenzene-1,2,4-triamine (**6c**). To a suspension of 5-chloro-*N*²-(4-((2-(dimethylamino)ethyl)(methyl)amino)-2-methoxy-5-nitrophenyl)-*N*⁴-(2-(isopropylsulfonyl)phenyl)pyrimidine-2,4-diamine (**5c**) (0.274 g, 0.473 mmol) and tin (II) chloride dihydrate (1.00 g, 4.74 mmol) in ethyl acetate (7 mL) was added conc. HCl (1 mL). Then, the resulting mixture was stirred at 50 °C for 5 h and quenched with NH₄OH (pH 5), Na₂CO₃ solid (pH 7) and the resulting suspension was filtered through Celite. The filtrate was concentrated under reduced pressure to afford **6c** as a brown solid (217 mg, 92 %). ¹H NMR (500 MHz, DMSO-*d*₆) δ 9.58 (s, 1H), 8.67 (d, *J* = 8.6 Hz, 1H), 8.32 (s, 1H), 8.20 (s, 1H), 7.80 (dd, *J* = 7.9, 1.5 Hz, 1H), 7.69 - 7.63 (m, 1H), 7.33 - 7.27 (m, 1H), 7.08 (bs, 1H), 6.81 (s, 1H),

3.70 (s, 3H), 3.49 - 3.39 (m, 1H), 3.27 (br t, $J = 6.0$ Hz, 2H), 3.19 (br t, $J = 5.8$ Hz, 2H), 2.80 (s, 6H), 2.55 (s, 3H), 1.17 (d, $J = 6.7$ Hz, 6H); LC/MS (ESI) m/z 548.58 $[M+H]^+$.

N-(5-((5-Chloro-4-((2-(isopropylsulfonyl)phenyl)amino)pyrimidin-2-yl)amino)-2-((2-(dimethylamino)ethyl)(methyl)amino)-4-methoxyphenyl)acrylamide (**7c**). To a solution of *N*⁴-(5-chloro-4-((2-(isopropylsulfonyl)phenyl)amino)pyrimidin-2-yl)-*N*¹-(2-(dimethylamino)ethyl)-5-methoxy-*N*¹-methylbenzene-1,2,4-triamine (**6c**) (120 mg, 0.219 mmol) in THF (2 mL) and aq.NaHCO₃ (2 mL) was added dropwise acryloyl chloride (0.027 mL, 0.329 mmol) at 0 °C. After stirring at 0 °C for 10 min, the reaction mixture was diluted with excess DCM and washed with brine. The organic layer was dried over Na₂SO₄, filtered and concentrated under reduced pressure. The residue was purified by preparative HPLC to give **7c** as an off-white solid (52 mg, 53 %). ¹H NMR (500 MHz, DMSO-*d*₆) δ 10.02 (br s, 1H), 9.52 (s, 1H), 8.57 - 8.46 (m, 2H), 8.39 (s, 1H), 8.22 (s, 1H), 7.76 (dd, $J = 7.9, 1.5$ Hz, 1H), 7.47 (t, $J = 7.0$ Hz, 1H), 7.23 (t, $J = 7.5$ Hz, 1H), 7.00 (s, 1H), 6.48 - 6.30 (m, 1H), 6.15 (dd, $J = 16.8, 1.8$ Hz, 1H), 5.72 (dd, $J = 10.2, 1.8$ Hz, 1H), 3.76 (s, 3H), 3.47 - 3.38 (m, 1H), 2.90 (br s, 2H), 2.71 (s, 3H), 2.36 (br s, 2H), 2.24 (br s, 6H), 1.16 (d, $J = 6.7$ Hz, 6H); ¹³C NMR (125 MHz, DMSO-*d*₆) δ 162.5, 158.5, 155.4, 154.5, 148.8, 140.1, 138.0, 134.5, 132.1, 130.8, 126.9, 126.2, 123.8, 123.4, 122.9, 122.9, 117.8, 105.4, 104.1, 56.7, 55.7, 54.9, 54.9, 45.1, 45.1, 42.2, 14.9, 14.9; LC/MS (ESI) m/z 602.69 $[M+H]^+$; HRMS (ESI) calcd for C₂₈H₃₇ClN₇O₄S $[M+H]^+$ 602.2311; found 602.2304.

4.1.1.1 *N*-(5-((5-chloro-4-((2-(isopropylsulfonyl)phenyl)amino)pyrimidin-2-yl)amino)-2-((2-(dimethylamino)ethyl)(methyl)amino)-4-methoxyphenyl)propionamide (**7c-R**). **7c-R** was synthesized using the analog method that used to synthesize **7c**. To a solution of *N*⁴-(5-chloro-4-

((2-(isopropylsulfonyl)phenyl)amino)pyrimidin-2-yl)-*N*¹-(2-(dimethylamino)ethyl)-5-methoxy-*N*¹-methylbenzene-1,2,4-triamine (**6c**) (35 mg, 0.064 mmol) in THF (1 mL) and aq.NaHCO₃ (1 mL) was added dropwise propionyl chloride (0.014 mL, 0.154 mmol) at 0 °C. After stirring at 0 °C for 10 min, the reaction mixture was diluted with excess DCM and washed with brine. The organic layer was dried over Na₂SO₄, filtered and concentrated under reduced pressure. The residue was purified by preparative HPLC to give **7c-R** as an off-white solid (28 mg, 72 %). ¹H NMR (500 MHz, DMSO-*d*₆) δ 9.64 (br s, 1H), 9.53 (s, 1H), 8.54 (d, *J* = 7.9 Hz, 1H), 8.48 (s, 1H), 8.22 (s, 1H), 7.78 (d, *J* = 7.9 Hz, 1H), 7.52 (br s, 1H), 7.26 (t, *J* = 7.5 Hz, 1H), 6.96 (s, 1H), 3.76 (s, 3H), 3.47 - 3.40 (m, 1H), 2.97 (br s, 2H), 2.68 (s, 3H), 2.60 - 2.05 (m, 10H), 1.17 (d, *J* = 6.7 Hz, 6H), 1.04 (t, *J* = 7.5 Hz, 3H); LC/MS (ESI) *m/z* 604.35 [M+H]⁺.

4.1.1.2

N-(2-((2-(Dimethylamino)ethyl)(methyl)amino)-5-((4-((2-(isopropylsulfonyl)phenyl)amino)pyrimidin-2-yl)amino)-4-methoxyphenyl)acrylamide (**7a**). The procedure that used to synthesize **7c** was applied to prepare **7a** from compound **1-1**. ¹H NMR (400 MHz, DMSO-*d*₆) δ 10.09 (br s, 1H), 8.87 (br s, 1H), 8.55 (br s, 1H), 8.19 (d, *J* = 8.2 Hz, 1H), 8.07 (d, *J* = 5.6 Hz, 1H), 7.97 (s, 1H), 7.77 - 7.75 (m, 1H), 7.54 (br t, *J* = 8.0 Hz, 1H), 7.24 (t, *J* = 7.9 Hz, 1H), 6.96 (s, 1H), 6.36 - 6.33 (m, 2H), 6.19 - 6.14 (m, 1H), 5.74 - 5.71 (m, 1H), 3.79 (s, 3H), 3.48 - 3.34 (m, 1H), 2.86 (br t, *J* = 6.5 Hz, 2H), 2.69 (s, 3H), 2.28 (br t, *J* = 6.5 Hz, 2H), 2.20 (s, 6H), 1.14 (d, *J* = 6.8 Hz, 6H); LC/MS (ESI) *m/z* 568.45 [M+H]⁺; HRMS (ESI) calcd for C₂₈H₃₈N₇O₄S [M+H]⁺ 568.2700; found 568.2695.

4.1.1.3

N-(2-((2-(Dimethylamino)ethyl)(methyl)amino)-5-((5-fluoro-4-((2-(isopropylsulfonyl)phenyl)amino)pyrimidin-2-yl)amino)-4-methoxyphenyl)acrylamide (**7b**). The

procedure that used to synthesize **7c** was applied to prepare **7b** from compound **1-2**. ¹H NMR (500 MHz, DMSO-*d*₆) δ 9.54 (br s, 1H), 9.45 (d, *J* = 2.1 Hz, 1H), 8.55 (d, *J* = 8.5 Hz, 1H), 8.30 (br, 1H), 8.19 (d, *J* = 3.1 Hz, 1H), 8.00 (s, 1H), 7.80 (dd, *J* = 7.9, 1.5 Hz, 1H), 7.61 - 7.57 (m, 1H), 7.29 - 7.24 (m, 1H), 6.96 (s, 1H), 6.61 - 6.52 (m, 1H), 6.23 (dd, *J* = 17.9, 1.5 Hz, 1H), 5.75 (dd, *J* = 10.4, 1.5 Hz, 1H), 3.84 (s, 3H), 3.50 - 3.42 (m, 1H), 3.16 (br, 3H), 3.01 (br, 2H), 2.69 - 2.62 (s, 8H), 1.18 (d, *J* = 6.7 Hz, 6H); LC/MS (ESI) *m/z* 586.72 [M+H]⁺; HRMS (ESI) calcd for C₂₈H₃₇FN₇O₄S [M+H]⁺ 586.2606; found 586.2596.

4.1.1.4 *N*-(2-((2-(Dimethylamino)ethyl)(methyl)amino)-5-((5-iodo-4-((2-(isopropylsulfonyl)phenyl)amino)pyrimidin-2-yl)amino)-4-methoxyphenyl)acrylamide (**7d**). The procedure that used to synthesize **7c** was applied to prepare **7d** from compound **1-4**. ¹H NMR (400 MHz, DMSO-*d*₆) δ 10.13 (br s, 1H), 9.13 (br s, 1H), 8.46 - 8.42 (m, 4H), 7.81 - 7.79 (m, 1H), 7.50 (br t, *J* = 7.3 Hz, 1H), 7.31 - 7.24 (m, 1H), 7.05 (s, 1H), 6.45 - 6.38 (m, 1H), 6.18 (m, 1H), 5.77 (m, 1H), 3.81 (s, 3H), 3.51 - 3.41 (m, 1H), 2.94 - 2.91 (m, 2H), 2.77 (s, 3H), 2.39 - 2.35 (m, 2H), 2.26 (s, 6H), 1.24 (d, *J* = 6.8 Hz, 6H); LC/MS (ESI) *m/z* 694.30 [M+H]⁺; HRMS (ESI) calcd for C₂₈H₃₇IN₇O₄S [M+H]⁺ 694.1667; found 694.1661.

4.1.1.5 *N*-(2-((2-(Dimethylamino)ethyl)(methyl)amino)-5-((4-((2-(*N,N*-dimethylsulfamoyl)phenyl)amino)pyrimidin-2-yl)amino)-4-methoxyphenyl)acrylamide (**7i**). The procedure that used to synthesize **7c** was applied to prepare **7i** from compounds **1-1** and **2-3**. ¹H NMR (400 MHz, CDCl₃) δ 10.06 (s, 1H), 8.73 (br s, 1H), 8.58 (br s, 1H), 8.16 (d, *J* = 8.0 Hz, 1H), 8.06 (d, *J* = 5.7 Hz, 1H), 7.91 (s, 1H), 7.72 - 7.69 (m, 1H), 7.46 (br t, *J* = 7.3 Hz, 1H), 7.20 (t, *J* = 7.4 Hz, 1H), 6.96 (s, 1H), 6.39 - 6.32 (m, 2H), 6.17 - 6.12 (m, 1H), 5.73 - 5.70 (m, 1H),

3.79 (s, 3H), 2.85 (br t, $J = 5.2$ Hz, 2H), 2.69 (s, 3H), 2.62 (s, 6H), 2.29 (br t, $J = 5.2$ Hz, 2H), 2.21 (s, 6H); LC/MS (ESI) m/z 569.45 $[M+H]^+$; HRMS (ESI) calcd for $C_{27}H_{37}N_8O_4S$ $[M+H]^+$ 569.2653; found 569.2649.

4.1.1.6

N-(2-((2-(Dimethylamino)ethyl)(methyl)amino)-5-((4-((2-(*N,N*-dimethylsulfamoyl)phenyl)amino)-5-fluoropyrimidin-2-yl)amino)-4-methoxyphenyl)acrylamide

(**7j**). The procedure that used to synthesize **7c** was applied to prepare **7j** from compounds **1-2** and **2-3**. 1H NMR (400 MHz, DMSO- d_6) δ 10.09 (br s, 1H), 9.28 (br s, 1H), 8.56 (d, $J = 8.3$ Hz, 1H), 8.50 (br s, 1H), 8.25 (s, 1H), 8.20 (s, 1H), 7.73 (d, $J = 8.0$ Hz, 1H), 7.47 (br t, $J = 7.6$ Hz, 1H), 7.22 (br t, $J = 7.6$ Hz, 1H), 6.99 (s, 1H), 6.44 - 6.37 (m, 1H), 6.16 (br d, $J = 16.9$ Hz, 1H), 5.74 (br d, $J = 10.2$ Hz, 1H) 3.78 (s, 3H), 2.89 (m, 2H), 2.70 (s, 3H), 2.51 (d, $J = 1.48$ Hz, 6H), 2.35 (m, 2H), 2.24 (s, 6H); LC/MS (ESI) m/z 587.20 $[M+H]^+$; HRMS (ESI) calcd for $C_{27}H_{36}FN_8O_4S$ $[M+H]^+$ 587.2559; found 587.2551.

4.1.1.7 *N*-(5-((5-Chloro-4-((2-(*N,N*-dimethylsulfamoyl)phenyl)amino)pyrimidin-2-yl)amino)-2-

((2-(dimethylamino)ethyl)(methyl)amino)-4-methoxyphenyl)acrylamide (**7k**). The procedure that used to synthesize **7c** was applied to prepare **7k** from compounds **1-3** and **2-3**. 1H NMR (400 MHz, DMSO- d_6) δ 10.08 (br s, 1H), 9.37 (br s, 1H), 8.51 - 8.48 (m, 2H) 8.42 (s, 1H), 8.22 (s, 1H), 7.73 - 7.71 (m, 1H), 7.41 (br t, $J = 8.0$ Hz, 1H), 7.20 (t, $J = 7.8$ Hz, 1H), 7.01 (s, 1H), 6.40 - 6.33 (m, 1H), 6.17 - 6.12 (m, 1H), 5.73 - 5.70 (m, 1H), 3.76 (s, 3H), 2.87 (br t, $J = 5.6$ Hz, 2H), 2.72 (s, 3H), 2.64 (s, 6H), 2.31 (br t, $J = 5.6$ Hz, 2H), 2.21 (s, 6H); LC/MS (ESI) m/z 603.45 $[M+H]^+$; HRMS (ESI) calcd for $C_{27}H_{36}ClN_8O_4S$ $[M+H]^+$ 603.2263; found 603.2256.

4.1.1.8

N-(2-((2-(*N,N*-dimethylamino)ethyl)(methylamino)-5-((4-((2-(*N,N*-

dimethylsulfamoyl)phenyl)amino)-5-iodopyrimidin-2-yl)amino)-4-methoxyphenyl)acrylamide

(**7l**). The procedure that used to synthesize **7c** was applied to prepare **7l** from compounds **1-4** and **2-3**. ¹H NMR (400 MHz, DMSO-*d*₆) δ 9.91 (s, 1H), 9.01 (s, 1H), 8.98 - 8.92 (m, 4H), 7.74 - 7.67 (m, 1H), 7.43 (br t, *J* = 7.7 Hz, 1H), 7.23 (t, *J* = 7.1 Hz, 1H), 6.94 (s, 1H), 6.63 - 6.60 (m, 1H), 6.15 - 6.11 (m, 1H), 5.73 - 5.69 (m, 1H), 3.77 (s, 3H), 3.08 - 3.06 (m, 2H), 2.80 (s, 3H), 2.40 - 2.38 (m, 2H), 2.20 (s, 6H), 1.23 (s, 6H); LC/MS (ESI) *m/z* 695.30 [M+H]⁺; HRMS (ESI) calcd for C₂₇H₃₆IN₈O₄S [M+H]⁺ 695.1619; found 695.1606.

4.1.2 Representative procedure for the synthesis of compounds **7e** - **7h**

(2-((2-Chloro-5-fluoropyrimidin-4-yl)amino)phenyl)dimethylphosphine oxide (**3f**). To a solution of 2,4-dichloro-5-fluoropyrimidine (0.5 g, 2.99 mmol) and (2-aminophenyl)dimethylphosphine oxide (0.323 g, 1.907 mmol) in DMF (6.36 mL) was added potassium carbonate (0.828 g, 5.99 mmol). The reaction mixture was stirred at 70 °C for overnight. After completion of the reaction, the resulting mixture was cooled to room temperature, quenched with water, extracted with DCM and washed with brine. The combined organic layer was dried over Na₂SO₄, filtered and concentrated under reduced pressure. The residue was purified by flash column chromatography on silica gel (0 to 20 % MeOH in DCM) to give **3f** as a yellowish solid (0.178 g, 31 %). ¹H NMR (400 MHz, DMSO-*d*₆) δ 12.09 (s, 1H), 8.54 - 8.51 (m, 1H), 8.37 (br d, *J* = 3.0 Hz, 1H), 7.68 - 7.60 (m, 2H), 7.23 (br t, *J* = 6.7 Hz, 1H), 1.83 (s, 3H), 1.80 (s, 3H); LC/MS (ESI) *m/z* 300.00 [M+H]⁺.

(2-((5-Fluoro-2-((4-fluoro-2-methoxy-5-nitrophenyl)amino)pyrimidin-4-yl)amino)phenyl)dimethylphosphine oxide (**4f**). To a solution of (2-((2-chloro-5-fluoropyrimidin-4-yl)amino)phenyl)dimethylphosphine oxide (**3f**) (0.1 g, 0.334 mmol) and 4-fluoro-2-methoxy-5-nitroaniline (0.124 g, 0.667 mmol) in *sec*-butanol (2 mL) was added potassium carbonate (0.231 g, 1.669 mmol). The reaction mixture was stirred at 80 °C for 10 min and then Pd₂(dba)₃ (0.031 g, 0.033 mmol) and Xphos (0.016 g, 0.033 mmol) were added rapidly. The reaction mixture was stirred at 100 °C for 2 h. After completion of the reaction, the resulting mixture was hot-filtered through Celite and washed with DCM. The filtrate was concentrated under reduced pressure and then purified by flash column chromatography on silica gel (0 to 20 % MeOH in DCM) to afford **4f** as a yellowish solid (0.128 g, 85 %). ¹H NMR (400 MHz, DMSO-*d*₆) δ 11.64 (s, 1H), 8.74 (d, *J* = 8.4 Hz, 1H), 8.63 - 8.60 (m, 1H), 8.38 (s, 1H), 8.18 (br d, *J* = 3.3 Hz, 1H), 7.60 - 7.55 (m, 1H), 7.40 (br t, *J* = 8.1 Hz, 1H), 7.33 (d, *J* = 13.4 Hz, 1H), 7.12 (br t, *J* = 7.2 Hz, 1H), 3.97 (s, 3H), 1.81 (s, 3H), 1.78 (s, 3H); LC/MS (ESI) *m/z* 450.05 [M+H]⁺.

(2-((2-((4-((2-(Dimethylamino)ethyl)(methyl)amino)-2-methoxy-5-nitrophenyl)amino)-5-fluoropyrimidin-4-yl)amino)phenyl)dimethylphosphine oxide (**5f**). To a solution of (2-((5-fluoro-2-((4-fluoro-2-methoxy-5-nitrophenyl)amino)pyrimidin-4-yl)amino)phenyl)dimethylphosphine oxide (**4f**) (0.128 g, 0.285 mmol) in dioxane (3 mL) was added *N*¹,*N*¹,*N*²-trimethylethane-1,2-diamine (0.362 mL, 2.85 mmol). After stirring at 100 °C for 2 h, the resulting mixture was concentrated under reduced pressure. The residue was purified by flash column chromatography on silica gel to give **5f** as a yellowish solid (0.151g, quantitative). ¹H NMR (400 MHz, DMSO-*d*₆) δ 11.55 (br s, 1H), 8.58 - 8.57 (m, 1H), 8.22 (s, 1H), 8.15 (s, 1H), 8.10 (br d, *J* = 3.3 Hz, 1H), 7.58 - 7.52 (m, 1H), 7.33 (br t, *J* = 7.7 Hz, 1H), 7.08 (br t, *J* = 6.7 Hz, 1H), 6.79 (s, 1H), 3.89 (s,

3H), 3.23 (br t, $J = 6.8$ Hz, 2H), 2.82 (s, 3H), 2.46 - 2.41 (m, 2H), 2.13 (s, 6H), 1.79 (s, 3H), 1.76 (s, 3H); LC/MS (ESI) m/z 532.15 $[M+H]^+$.

(2-((2-((5-Amino-4-((2-(dimethylamino)ethyl)(methyl)amino)-2-methoxyphenyl)amino)-5-fluoropyrimidin-4-yl)amino)phenyl)dimethylphosphine oxide (**6f**). To a solution of 2-((2-((4-((2-(dimethylamino)ethyl)(methyl)amino)-2-methoxy-5-nitrophenyl)amino)-5-fluoropyrimidin-4-yl)amino)phenyl)dimethylphosphine oxide (**5f**) (0.151 g, 0.284 mmol) in MeOH (20 mL) was added 10 % Pd/C (0.02 g, 0.019 mmol). The reaction mixture was stirred at room temperature under an atmosphere of H₂ for overnight. After completion of the reaction, the resulting mixture was filtered through Celite, and was washed with methanol. The filtrate was concentrated under reduced pressure to afford **6f** as a yellowish solid (0.142 g, quantitative). ¹H NMR (400 MHz, DMSO-*d*₆) δ 11.46 (br s, 1H), 8.68 - 8.65 (m, 1H), 8.04 (br d, $J = 3.4$ Hz, 1H), 7.82 (s, 1H), 7.57 - 7.51 (m, 1H), 7.45 (br t, $J = 8.0$ Hz, 1H), 7.13 (s, 1H), 7.08 (br t, $J = 7.4$ Hz, 1H), 6.72 (s, 1H), 3.68 (s, 3H), 2.97 - 2.94 (m, 2H), 2.57 (s, 3H), 2.35 (br s, 6H), 1.79 (s, 3H), 1.75 (s, 3H); LC/MS (ESI) m/z 502.15 $[M+H]^+$.

N-(2-((2-(Dimethylamino)ethyl)(methyl)amino)-5-((4-((2-(dimethylphosphoryl)phenyl)amino)-5-fluoropyrimidin-2-yl)amino)-4-methoxyphenyl)acrylamide trifluoroacetate salt (**7f**). To a solution of (2-((2-((5-amino-4-((2-(dimethylamino)ethyl)(methyl)amino)-2-methoxyphenyl)amino)-5-fluoropyrimidin-4-yl)amino)phenyl)dimethylphosphine oxide (**6f**) (0.142 g, 0.283 mmol) in THF (5 mL) and aq.NaHCO₃ (5 mL) was added dropwise acryloyl chloride (0.034 mL, 0.425 mmol) at 0 °C. After stirring for 10 min, the resulting mixture was diluted with DCM and washed with brine. The organic layer was dried over Na₂SO₄, filtered and

concentrated under reduced pressure. The residue was purified by preparative HPLC to give **7f** as a yellowish solid (0.037 g, 23 %). ¹H NMR (400 MHz, DMSO-*d*₆) δ 11.83 (br d, *J* = 19.5 Hz, 1H), 9.58 (s, 1H), 9.25 (br s, 1H), 8.64 (br s, 1H), 8.53 - 8.51 (m, 1H), 8.15 - 8.13 (m, 2H), 7.60 - 7.55 (m, 1H), 7.37 (br t, *J* = 7.8 Hz, 1H), 7.10 (br t, *J* = 7.7 Hz, 1H), 6.98 (s, 1H), 6.63 - 6.56 (m, 1H), 6.28 (d, *J* = 16.8 Hz, 1H), 5.79 (d, *J* = 10.2 Hz, 1H), 3.83 (s, 3H), 3.29 - 3.24 (m, 4H), 2.78 (s, 6H), 2.59 (s, 3H), 1.80 (s, 3H), 1.77 (s, 3H); LC/MS (ESI) *m/z* 556.30 [M+H]⁺; HRMS (ESI) calcd for C₂₇H₃₆FN₇O₃P [M+H]⁺ 556.2596; found 556.2592.

4.1.2.1

N-(2-((2-(Dimethylamino)ethyl)(methyl)amino)-5-((4-((2-(dimethylphosphoryl)phenyl)amino)pyrimidin-2-yl)amino)-4-methoxyphenyl)acrylamide

trifluoroacetate salt (**7e**). The procedure that used to synthesize **7f** was applied to prepare **7e** from compound **1-1**. ¹H NMR (400 MHz, CD₃OD) δ 8.04 (br s, 1H), 7.90 (br d, *J* = 6.0 Hz, 1H), 7.72 - 7.67 (m, 2H), 7.56 (br t, *J* = 7.5 Hz, 1H), 7.37 (br t, *J* = 7.4 Hz, 1H), 6.99 (s, 1H), 6.54 - 6.49 (m, 2H), 6.41 (d, *J* = 7.2 Hz, 1H), 5.92 - 5.90 (m, 1H), 3.95 (s, 3H), 3.51 - 3.47 (m, 2H), 3.28 - 3.25 (m, 2H), 2.87 (s, 6H), 2.71 (s, 3H), 1.86 (s, 3H), 1.83 (s, 3H); LC/MS (ESI) *m/z* 538.15 [M+H]⁺; HRMS (ESI) calcd for C₂₇H₃₇N₇O₃P [M+H]⁺ 538.2690; found 538.2689.

4.1.2.2

N-(5-((5-Chloro-4-((2-(dimethylphosphoryl)phenyl)amino)pyrimidin-2-yl)amino)-2-((2-(dimethylamino)ethyl)(methyl)amino)-4-methoxyphenyl)acrylamide trifluoroacetate salt (**7g**).

The procedure that used to synthesize **7f** was applied to prepare **7g** from compound **1-3**. ¹H NMR (400 MHz, DMSO-*d*₆) δ 11.30 (s, 1H), 9.57 (s, 1H), 9.20 (br s, 1H), 8.43 - 8.41 (m, 2H), 8.15 (s, 1H), 8.08 (s, 1H), 7.57 - 7.51 (m, 1H), 7.33 (br t, *J* = 7.8 Hz, 1H), 7.06 (br t, *J* = 7.2 Hz, 1H), 6.98 (s, 1H), 6.62 - 6.56 (m, 1H), 6.31 - 6.26 (m, 1H), 5.81 - 5.78 (m, 1H), 3.83 (s, 3H),

3.30 - 3.24 (m, 4H), 2.79 (br s, 6H), 2.59 (s, 3H), 1.78 (s, 3H), 1.74 (s, 3H); LC/MS (ESI) m/z 573.10 $[M+H]^+$; HRMS (ESI) calcd for $C_{27}H_{36}N_7O_3P$ $[M+H]^+$ 572.2300; found 572.2294.

4.1.2.3

N-(2-((2-(Dimethylamino)ethyl)(methyl)amino)-5-((4-((2-(dimethylphosphoryl)phenyl)amino)-5-iodopyrimidin-2-yl)amino)-4-methoxyphenyl)acrylamide trifluoroacetate salt (**7h**). The procedure that used to synthesize **7f** was applied to prepare **7h** from compound **1-4**. 1H NMR (400 MHz, DMSO- d_6) δ 10.70 (br s, 1H), 9.55 (s, 1H), 9.24 (br s, 1H), 8.45 - 8.43 (m, 1H), 8.33 (s, 1H), 8.13 - 8.10 (m, 1H), 8.05 (s, 1H), 7.55 - 7.50 (m, 1H), 7.33 (br t, $J = 7.8$ Hz, 1H), 7.07 (br t, $J = 8.0$ Hz, 1H), 6.96 (s, 1H), 6.64 - 6.57 (m, 1H), 6.31 - 6.26 (m, 1H), 5.82 - 5.79 (m, 1H), 3.82 (s, 3H), 3.28 - 3.22 (m, 4H), 2.78 (br d, $J = 4.6$ Hz, 6H), 2.57 (s, 3H), 1.76 (s, 3H), 1.73 (s, 3H); LC/MS (ESI) m/z 664.00 $[M+H]^+$; HRMS (ESI) calcd for $C_{27}H_{36}N_7O_3P$ $[M+H]^+$ 664.1656; found 664.1645.

4.2 Pharmacology

4.2.1 Enzymatic assays

The enzymatic activity against ALK was tested using Z'-Lyte assay with the ATP concentration equal to the apparent K_m . The protocol is available from Life Technologies. All EGFR kinase inhibition assays were conducted by using Promega ADP-Glo Kinase assay systems (Catalog number; V4507, V5325, and V9261). Final compound concentrations were 50 μ M, 5 μ M, 500 nM, 50 nM, 5 nM, 500 pM, 50 pM, 5 pM, and 0.5 pM and performed at each concentration with osimertinib as a positive control. Each compound was mixed with 0.2 μ g/uL

of substrate (Poly G:T (4:1) (Signal Chem, Richmond, BC, Canada)), 5 $\mu\text{mol/L}$ ATP (Invitrogen, Carlsbad, CA), 5 ng of EGFR enzyme, and kinase reaction buffer (40 mmol/L TrisHCl, 10 mmol/L MgCl_2 , and 0.1 $\mu\text{g}/\mu\text{L}$ BSA(bovine serum albumin)) in 384-well plate. After 30 min reaction at room temperature, ADP-Glo (Promega, Madison, WI) reagent was added and incubated at room temperature for 40 min. Finally, Kinase Detection Reagent was added and reacted at room temperature for 30 min. The luminescence signals were detected by using a microplate ELISA reader (Bio-Tek). Compound inhibition curves were fitted using Graphpad Prism 6.0 software.

4.2.2 Cell lines and cell growth inhibition assay

The NSCLC cell lines DFCI032 (*EML4-ALK* variant 1 E13:A20), and DFCI076 (*EML4-ALK* variant 3 E6:A20) have been previously published [14, 33]. DFCI032 and DFCI076 were established at Dana-Farber Cancer Institute from patients with crizotinib resistance and were cultured in ACL-4 media (Life Technologies) supplemented with 10% FBS, 100 units/mL penicillin, 100mg/mL streptomycin. *EML4-ALK* variant 1, wild type EGFR, L858R, exon19del, T790M/L858R and T790M/exon19del transformed Ba/F3 cells were established as previously described [14, 24, 35] and maintained in complete RPMI 1640 media without IL-3. Parental Ba/F3 cells and wildtype EGFR Ba/F3 cells were grown in complete RPMI 1640 media in the presence of IL-3 or EGF, respectively.

Ba/F3 cells and NSCLC cells were treated with dose-escalated drug over the course of 72 hours. Growth and inhibition of growth was assessed by MTS assay according to previously

established methods. All experimental treatments were performed in replicates (6-12 wells per treatment) and the presented data are representative of the replicates. The data was graphically displayed using GraphPad Prism version 5.0 for Windows. The EC₅₀ values were fitted using a non-linear regression model with a sigmoidal dose response.

4.2.3 *Antibodies and Western blotting*

Cell lysis and Western blotting were done as previously described [24]. Antibodies against total-ALK (D5F3), phospho-ALK (Tyr-1604), phospho-EGFR (Tyr-1068; #3777), phospho-Akt (Ser-473; D9E), total-Akt, Total-ERK1/2 and phospho-ERK1/2 (pT185/pY187) were obtained from Cell Signaling Technology; total-EGFR from Bethyl Laboratories; α -tubulin from Sigma Aldrich.

4.2.4 *Kinome selectivity profiling*

Kinome selectivity profiling was performed using the KINOMEScan method at a compound concentration of 1 μ M. Protocols are available from DiscoverX.

4.2.5 *Liver microsomal stability test*

Acetaminophen, chlorpropamide, dextromethorphan, dextrorphan, phenacetin, and tolbutamide were purchased from Sigma-Aldrich (St. Louis, MO). Pooled human liver microsomes (150 donor) and dog, rat, mouse liver microsomes were obtained from BD Gentest

Co. (Woburn, MA). NADPH regeneration system was obtained from Promega. S-Mephenytoin, 4-hydroxymephenytoin, 1'-hydroxymidazolam were purchased from Ultrafine Chemical Co. (Manchester, UK). All other chemicals and solvents were of the highest grade available. The liver microsomal stability assay was performed by incubation of human and selected animal liver microsomes at 37 °C with a test compound at a final concentration of 1 µM, in the presence of 0.5 mg/mL microsomal protein and NADPH regeneration system, in a total volume of 100 µL of 100 mM phosphate buffer, pH 7.4. The incubation was started by the addition of NADPH regeneration system and terminated with 40 µL of ice-cold acetonitrile at 0 and 30 min. Precipitated proteins were removed by centrifugation at 10,000×g for 5 min at 4 °C. Aliquots of the supernatant were injected onto an LC-MS/MS system. Incubations terminated prior to the addition of the NADPH regeneration system (time point 0 min) were used as standards, defined as 100 %. Percent of the parent compound remaining is calculated by comparing peak areas.

4.2.6 Cytochrome P450 inhibition assay

All incubations were performed in duplicate and the mean values were used for analysis. The assays of phenacetin O-deethylase, tolbutamide 4-hydroxylase, S-mephenytoin 4-hydroxylase, dextromethorphan O-demethylase and midazolam 1'-hydroxylase activities were determined as probe activities for CYP1A2, CYP2C9, CYP2C19, CYP2D6 and CYP3A, respectively, using cocktail incubation and tandem mass spectrometry. Briefly, incubation reaction was performed with 0.25 mg/mL human liver microsomes in a final incubation volume of 100 µL. The incubation medium contained 100 mM phosphate buffer (pH 7.4) with probe substrates. The incubation mixture containing various inhibitors (10 µM) was pre-incubated for 5 min. After pre-incubation, an NADPH regenerating system was added. After incubation at 37 °C

for 15 min, the reaction was stopped by placing the incubation tubes on ice and adding 40 μ L of ice-cold acetonitrile. The incubation mixtures were then centrifuged at 10,000 \times g for 5 min at 4 $^{\circ}$ C. Aliquots of the supernatant were injected onto an LC-MS/MS system. The CYP-mediated activities in the presence of inhibitors were expressed as percentages of the corresponding control values.

Acknowledgment

This work was supported by a grant of the Daegu-Gyeongbuk Medical Innovation Foundation New Drug Development Center R&D Project.

Appendix A. Supplementary data

Supplementary data related to this article can be found at XXXX

Contains the biochemical activities of ceritinib and WZ4002 against EGFR T790M/L858R in the Z'-LYTE assay, the antiproliferative activity of **7c-R** against L858R and T790M/L858R EGFR transformed Ba/F3 cells, the biochemical activity of **7c** against potential additional targets, and the full KINOMEscan data of **7c**.

References

[1] M.A. Lemmon, J. Schlessinger, Cell signaling by receptor tyrosine kinases, *Cell*, 141 (2010) 1117-1134.

- [2] T.S. Mok, Personalized medicine in lung cancer: what we need to know, *Nat. Rev. Clin. Oncol.* 8 (2011) 661-668.
- [3] B.A. Chan, B.G. Hughes, Targeted therapy for non-small cell lung cancer: current standards and the promise of the future, *Transl. Lung Cancer Res.* 4 (2015) 36-54.
- [4] E.L. Kwak, Y.-J. Bang, D.R. Camidge, A.T. Shaw, B. Solomon, R.G. Maki, S.-H.I. Ou, B.J. Dezube, P.A. Jänne, D.B. Costa, M. Varella-Garcia, W.-H. Kim, T.J. Lynch, P. Fidias, H. Stubbs, J.A. Engelman, L.V. Sequist, W. Tan, L. Gandhi, M. Mino-Kenudson, G.C. Wei, S.M. Shreeve, M.J. Ratain, J. Settleman, J.G. Christensen, D.A. Haber, K. Wilner, R. Salgia, G.I. Shapiro, J.W. Clark, A.J. Iafrate, Anaplastic Lymphoma Kinase Inhibition in Non-Small-Cell Lung Cancer, *N. Engl. J. Med.* 363 (2010) 1693-1703.
- [5] T.J. Lynch, D.W. Bell, R. Sordella, S. Gurubhagavatula, R.A. Okimoto, B.W. Brannigan, P.L. Harris, S.M. Haserlat, J.G. Supko, F.G. Haluska, D.N. Louis, D.C. Christiani, J. Settleman, D.A. Haber, Activating mutations in the epidermal growth factor receptor underlying responsiveness of non-small-cell lung cancer to gefitinib, *N. Engl. J. Med.* 350 (2004) 2129-2139.
- [6] S. Khozin, G.M. Blumenthal, X. Jiang, K. He, K. Boyd, A. Murgo, R. Justice, P. Keegan, R. Pazdur, U.S. Food and Drug Administration approval summary: Erlotinib for the first-line treatment of metastatic non-small cell lung cancer with epidermal growth factor receptor exon 19 deletions or exon 21 (L858R) substitution mutations, *Oncologist*, 19 (2014) 774-779.
- [7] F. Solca, G. Dahl, A. Zoephel, G. Bader, M. Sanderson, C. Klein, O. Kraemer, F. Himmelsbach, E. Haaksma, G.R. Adolf, Target binding properties and cellular activity of afatinib (BIBW 2992), an irreversible ErbB family blocker, *J. Pharmacol. Exp. Ther.* 343 (2012) 342-350.

- [8] A.T. Shaw, D.W. Kim, R. Mehra, D.S. Tan, E. Felip, L.Q. Chow, D.R. Camidge, J. Vansteenkiste, S. Sharma, T. De Pas, G.J. Riely, B.J. Solomon, J. Wolf, M. Thomas, M. Schuler, G. Liu, A. Santoro, Y.Y. Lau, M. Goldwasser, A.L. Boral, J.A. Engelman, Ceritinib in ALK-rearranged non-small-cell lung cancer, *N. Engl. J. Med.* 370 (2014) 1189-1197.
- [9] E. Larkins, G.M. Blumenthal, H. Chen, K. He, R. Agarwal, G. Gieser, O. Stephens, E. Zahalka, K. Ringgold, W. Helms, S. Shord, J. Yu, H. Zhao, G. Davis, A.E. McKee, P. Keegan, R. Pazdur, FDA Approval: Alectinib for the Treatment of Metastatic, ALK-Positive Non-Small Cell Lung Cancer Following Crizotinib, *Clin. Cancer Res.* 22 (2016) 5171-5176.
- [10] S.N. Gettinger, L.A. Bazhenova, C.J. Langer, R. Salgia, K.A. Gold, R. Rosell, A.T. Shaw, G.J. Weiss, M. Tugnait, N.I. Narasimhan, D.J. Dorer, D. Kerstein, V.M. Rivera, T. Clackson, F.G. Haluska, D.R. Camidge, Activity and safety of brigatinib in ALK-rearranged non-small-cell lung cancer and other malignancies: a single-arm, open-label, phase 1/2 trial, *Lancet Oncol.* 17 (2016) 1683-1696.
- [11] P.A. Jänne, J.C. Yang, D.W. Kim, D. Planchard, Y. Ohe, S.S. Ramalingam, M.J. Ahn, S.W. Kim, W.C. Su, L. Horn, D. Haggstrom, E. Felip, J.H. Kim, P. Frewer, M. Cantarini, K.H. Brown, P.A. Dickinson, S. Ghiorghiu, M. Ranson, AZD9291 in EGFR inhibitor-resistant non-small-cell lung cancer, *N. Engl. J. Med.* 372 (2015) 1689-1699.
- [12] D.A. Cross, S.E. Ashton, S. Ghiorghiu, C. Eberlein, C.A. Nebhan, P.J. Spitzler, J.P. Orme, M.R. Finlay, R.A. Ward, M.J. Mellor, G. Hughes, A. Rahi, V.N. Jacobs, M. Red Brewer, E. Ichihara, J. Sun, H. Jin, P. Ballard, K. Al-Kadhimi, R. Rowlinson, T. Klinowska, G.H. Richmond, M. Cantarini, D.W. Kim, M.R. Ranson, W. Pao, AZD9291, an irreversible EGFR TKI, overcomes T790M-mediated resistance to EGFR inhibitors in lung cancer, *Cancer Discov.* 4 (2014) 1046-1061.

- [13] M.R. Finlay, M. Anderton, S. Ashton, P. Ballard, P.A. Bethel, M.R. Box, R.H. Bradbury, S.J. Brown, S. Butterworth, A. Campbell, C. Chorley, N. Colclough, D.A. Cross, G.S. Currie, M. Grist, L. Hassall, G.B. Hill, D. James, M. James, P. Kemmitt, T. Klinowska, G. Lamont, S.G. Lamont, N. Martin, H.L. McFarland, M.J. Mellor, J.P. Orme, D. Perkins, P. Perkins, G. Richmond, P. Smith, R.A. Ward, M.J. Waring, D. Whittaker, S. Wells, G.L. Wrigley, Discovery of a potent and selective EGFR inhibitor (AZD9291) of both sensitizing and T790M resistance mutations that spares the wild type form of the receptor, *J. Med. Chem.* 57 (2014) 8249-8267.
- [14] T. Sasaki, J. Koivunen, A. Ogino, M. Yanagita, S. Nikiforow, W. Zheng, C. Lathan, J.P. Marcoux, J. Du, K. Okuda, M. Capelletti, T. Shimamura, D. Ercan, M. Stumpfova, Y. Xiao, S. Weremowicz, M. Butaney, S. Heon, K. Wilner, J.G. Christensen, M.J. Eck, K.K. Wong, N. Lindeman, N.S. Gray, S.J. Rodig, P.A. Janne, A novel ALK secondary mutation and EGFR signaling cause resistance to ALK kinase inhibitors, *Cancer Res.* 71 (2011) 6051-6060.
- [15] T. Tani, H. Yasuda, J. Hamamoto, A. Kuroda, D. Arai, K. Ishioka, K. Ohgino, M. Miyawaki, I. Kawada, K. Naoki, Y. Hayashi, T. Betsuyaku, K. Soejima, Activation of EGFR Bypass Signaling by TGF α Overexpression Induces Acquired Resistance to Alectinib in ALK-Translocated Lung Cancer Cells, *Mol. Cancer Ther.* 15 (2016) 162-171.
- [16] M. Miyawaki, H. Yasuda, T. Tani, J. Hamamoto, D. Arai, K. Ishioka, K. Ohgino, S. Nukaga, T. Hirano, I. Kawada, K. Naoki, Y. Hayashi, T. Betsuyaku, K. Soejima, Overcoming EGFR bypass signal-induced acquired resistance to ALK tyrosine kinase inhibitors in ALK-translocated lung cancer, *Mol. Cancer Res.* 15 (2017) 106-114.
- [17] J.J. Yang, X.C. Zhang, J. Su, C.R. Xu, Q. Zhou, H.X. Tian, Z. Xie, H.J. Chen, Y.S. Huang, B.Y. Jiang, Z. Wang, B.C. Wang, X.N. Yang, W.Z. Zhong, Q. Nie, R.Q. Liao, T.S. Mok, Y.L. Wu, Lung cancers with concomitant EGFR mutations and ALK rearrangements: diverse

responses to EGFR-TKI and crizotinib in relation to diverse receptors phosphorylation, *Clin. Cancer Res.* 20 (2014) 1383-1392.

[18] H. Tanaka, A. Hayashi, T. Morimoto, K. Taima, Y. Tanaka, M. Shimada, A. Kurosea, S. Takanashi, K. Okumura, A case of lung adenocarcinoma harboring EGFR mutation and EML4-ALK fusion gene, *BMC Cancer*, 12 (2012) 558-561.

[19] C.S. Baik, M.C. Chamberlain, L.Q. Chow, Targeted Therapy for Brain Metastases in EGFR-Mutated and ALK-Rearranged Non-Small-Cell Lung Cancer, *J. Thorac. Oncol.* 10 (2015) 1268-1278.

[20] W. Cai, D. Lin, C. Wu, X. Li, C. Zhao, L. Zheng, S. Chuai, K. Fei, C. Zhou, F.R. Hirsch, Intratumoral Heterogeneity of ALK-Rearranged and ALK/EGFR Coaltered Lung Adenocarcinoma, *J. Clin. Oncol.* 33 (2015) 3701-3709.

[21] T.H. Marsilje, W. Pei, B. Chen, W. Lu, T. Uno, Y. Jin, T. Jiang, S. Kim, N. Li, M. Warmuth, Y. Sarkisova, F. Sun, A. Steffy, A.C. Pferdekamper, A.G. Li, S.B. Joseph, Y. Kim, B. Liu, T. Tuntland, X. Cui, N.S. Gray, R. Steensma, Y. Wan, J. Jiang, G. Chopiuk, J. Li, W.P. Gordon, W. Richmond, K. Johnson, J. Chang, T. Groessl, Y.Q. He, A. Phimister, A. Aycinena, C.C. Lee, B. Bursulaya, D.S. Karanewsky, H.M. Seidel, J.L. Harris, P.Y. Michellys, Synthesis, structure-activity relationships, and in vivo efficacy of the novel potent and selective anaplastic lymphoma kinase (ALK) inhibitor 5-chloro-N2-(2-isopropoxy-5-methyl-4-(piperidin-4-yl)phenyl)-N4-(2-(isopropylsulf onyl)phenyl)pyrimidine-2,4-diamine (LDK378) currently in phase 1 and phase 2 clinical trials, *J. Med. Chem.* 56 (2013) 5675-5690.

[22] A.V. Galkin, J.S. Melnick, S. Kim, T.L. Hood, N. Li, L. Li, G. Xia, R. Steensma, G. Chopiuk, J. Jiang, Y. Wan, P. Ding, Y. Liu, F. Sun, P.G. Schultz, N.S. Gray, M. Warmuth,

Identification of NVP-TAE684, a potent, selective, and efficacious inhibitor of NPM-ALK, *Proc. Natl. Acad. Sci. U S A*, 104 (2007) 270-275.

[23] W.S. Huang, S. Liu, D. Zou, M. Thomas, Y. Wang, T. Zhou, J. Romero, A. Kohlmann, F. Li, J. Qi, L. Cai, T.A. Dwight, Y. Xu, R. Xu, R. Dodd, A. Toms, L. Parillon, X. Lu, R. Anjum, S. Zhang, F. Wang, J. Keats, S.D. Wardwell, Y. Ning, Q. Xu, L.E. Moran, Q.K. Mohemmad, H.G. Jang, T. Clackson, N.I. Narasimhan, V.M. Rivera, X. Zhu, D. Dalgarno, W.C. Shakespeare, Discovery of Brigatinib (AP26113), a Phosphine Oxide-Containing, Potent, Orally Active Inhibitor of Anaplastic Lymphoma Kinase, *J. Med. Chem.* 59 (2016) 4948-4964.

[24] W. Zhou, D. Ercan, L. Chen, C.H. Yun, D. Li, M. Capelletti, A.B. Cortot, L. Chirieac, R.E. Jacob, R. Padera, J.R. Engen, K.K. Wong, M.J. Eck, N.S. Gray, P.A. Janne, Novel mutant-selective EGFR kinase inhibitors against EGFR T790M, *Nature*, 462 (2009) 1070-1074.

[25] L.V. Sequist, J.C. Soria, J.W. Goldman, H.A. Wakelee, S.M. Gadgeel, A. Varga, V. Papadimitrakopoulou, B.J. Solomon, G.R. Oxnard, R. Dziadziuszko, D.L. Aisner, R.C. Doebele, C. Galasso, E.B. Garon, R.S. Heist, J. Logan, J.W. Neal, M.A. Mendenhall, S. Nichols, Z. Piotrowska, A.J. Wozniak, M. Raponi, C.A. Karlovich, S. Jaw-Tsai, J. Isaacson, D. Despain, S.L. Matheny, L. Rolfe, A.R. Allen, D.R. Camidge, Rocicetinib in EGFR-mutated non-small-cell lung cancer, *N. Engl. J. Med.* 372 (2015) 1700-1709.

[26] A.O. Walter, R.T. Sjin, H.J. Haringsma, K. Ohashi, J. Sun, K. Lee, A. Dubrovskiy, M. Labenski, Z. Zhu, Z. Wang, M. Sheets, T. St Martin, R. Karp, D. van Kalken, P. Chaturvedi, D. Niu, M. Nacht, R.C. Petter, W. Westlin, K. Lin, S. Jaw-Tsai, M. Raponi, T. Van Dyke, J. Etter, Z. Weaver, W. Pao, J. Singh, A.D. Simmons, T.C. Harding, A. Allen, Discovery of a mutant-selective covalent inhibitor of EGFR that overcomes T790M-mediated resistance in NSCLC, *Cancer Discov.* 3 (2013) 1404-1415.

- [27] M. Warmuth, S. Kim, X.J. Gu, G. Xia, F. Adrian, Ba/F3 cells and their use in kinase drug discovery, *Curr. Opin. Oncol.* 19 (2007) 55-60.
- [28] H. Shao, S. Shi, S. Huang, A.J. Hole, A.Y. Abbas, S. Baumli, X. Liu, F. Lam, D.W. Foley, P.M. Fischer, M. Noble, J.A. Endicott, C. Pepper, S. Wang, Substituted 4-(thiazol-5-yl)-2-(phenylamino)pyrimidines are highly active CDK9 inhibitors: synthesis, X-ray crystal structures, structure-activity relationship, and anticancer activities, *J. Med. Chem.* 56 (2013) 640-659.
- [29] A. Lange, M. Gunther, F.M. Buttner, M.O. Zimmermann, J. Heidrich, S. Hennig, S. Zahn, C. Schall, A. Sievers-Engler, F. Ansideri, P. Koch, M. Laemmerhofer, T. Stehle, S.A. Laufer, F.M. Boeckler, Targeting the Gatekeeper MET146 of C-Jun N-Terminal Kinase 3 Induces a Bivalent Halogen/Chalcogen Bond, *J. Am. Chem. Soc.* 137 (2015) 14640-14652.
- [30] W. Zhou, D. Ercan, P.A. Janne, N.S. Gray, Discovery of selective irreversible inhibitors for EGFR-T790M, *Bioorg. Med. Chem. Lett.* 21 (2011) 638-643.
- [31] M.W. Karaman, S. Herrgard, D.K. Treiber, P. Gallant, C.E. Atteridge, B.T. Campbell, K.W. Chan, P. Ciceri, M.I. Davis, P.T. Edeen, R. Faraoni, M. Floyd, J.P. Hunt, D.J. Lockhart, Z.V. Milanov, M.J. Morrison, G. Pallares, H.K. Patel, S. Pritchard, L.M. Wodicka, P.P. Zarrinkar, A quantitative analysis of kinase inhibitor selectivity, *Nat. Biotechnol.* 26 (2008) 127-132.
- [32] D.M. Goldstein, N.S. Gray, P.P. Zarrinkar, High-throughput kinase profiling as a platform for drug discovery, *Nat. Rev. Drug Discov.* 7 (2008) 391-397.
- [33] J.P. Koivunen, C. Mermel, K. Zejnullahu, C. Murphy, E. Lifshits, A.J. Holmes, H.G. Choi, J. Kim, D. Chiang, R. Thomas, J. Lee, W.G. Richards, D.J. Sugarbaker, C. Ducko, N. Lindeman, J.P. Marcoux, J.A. Engelman, N.S. Gray, C. Lee, M. Meyerson, P.A. Janne, EML4-ALK fusion gene and efficacy of an ALK kinase inhibitor in lung cancer, *Clin. Cancer Res.* 14 (2008) 4275-4283.

[34] J.M. Hatcher, M. Bahcall, H.G. Choi, Y. Gao, T. Sim, R. George, P.A. Jänne, N.S. Gray, Discovery of Inhibitors That Overcome the G1202R Anaplastic Lymphoma Kinase Resistance Mutation, *J. Med. Chem.* 58 (2015) 9296-9308.

[35] J. Jiang, H. Greulich, P.A. Janne, W.R. Sellers, M. Meyerson, J.D. Griffin, Epidermal growth factor-independent transformation of Ba/F3 cells with cancer-derived epidermal growth factor receptor mutants induces gefitinib-sensitive cell cycle progression, *Cancer Res.* 65 (2005) 8968-8974.

Highlights

- Dual inhibitors of ALK/EGFR, particularly the T790M mutant, were rationally designed.
- Potencies of compounds were assessed using both enzymatic and cellular assays.
- **7c** displayed remarkable inhibitory activities against both ALK and EGFR.
- **7c** inhibited the growth of DFCI032 cells harboring EML4-ALK and activated EGFR.